

A new picture for 4-dimensional ‘spacetime’ from intersecting D-branes on the T^9

Tassilo Ott[†]

Instituut voor Theoretische Fysica, Katholieke Universiteit Leuven,
Celestijnenlaan 200D B-3001 Leuven, Belgium.

Abstract

A factorization of spacetime of the form $time \times \mathcal{M}^3 \times \mathcal{M}^3 \times \mathcal{M}^3$ is considered in this paper as the closed string background in type IIA. The idea behind this construction is that each \mathcal{M}^3 might give rise to one large spatial dimension of 4-dimensional spacetime in the closed string sector. In the open string sector, intersecting D6-branes can be constructed for the simple choice of an orientifolded $\mathcal{M}^3 = T^3$ in a similar way as on the prominent $T^6 = T^2 \times T^2 \times T^2$ using exact CFT. The D6-branes then are allowed to span general 2-cycles on each T_i^3 . The intersection 1-cycles between two stacks of branes on one T_i^3 can be understood as one spatial dimension of the effective 4-dimensional ‘spacetime’ for the massless chiral fermions charged under these two stacks. Additionally to the known solutions to the R-R tadpole equations conserving (3+1)-dimensional Poincare invariance, this allows for solutions with globally just (2+1)- or (1+1)-Poincare invariance. For non-supersymmetric solutions, a string tree-level and one-loop potential for the scalar moduli (including the spacetime radii) is generated in the NS-NS sector. This potential here is interpreted dynamically for radii and dilaton in order to describe the global evolution of the universe. In the late time picture, (3+1)-dimensional global Poincare invariance can be restored well within experimental bounds. This approach links particle properties (the chiral massless fermion spectrum) directly to the global evolution of the universe by the scalar potential, both depending on the same topological wrapping numbers. In the future, this might lead to much better falsifiable phenomenological models.

[†] tassilo.ott@fys.kuleuven.be

1 Introduction

All matter of the standard model is chiral and appears in bifundamental representations of unitary and special unitary gauge factors.

In 1996, Berkooz, Douglas and Leigh discovered that intersecting D-branes in general lead to chiral fermions in the massless open string sector when embedded in a closed string type IIA string theory [1]. Bifundamental massless fermions in this picture correspond to strings, stretching between two stacks of D-branes and then shrinking to zero size¹. Every stack of D-branes (with a stacksize N) gives rise to a unitary gauge factor $U(N)$. The bifundamental representations of chiral fermions then are of the type (N_a, \bar{N}_b) or (N_a, N_b) , where a is the stack where the one endpoint and b the second stack where the other endpoint of the open string lies.

Many phenomenological models have been constructed in the meanwhile (for an overview see for instance [2–6]), and in all these constructions (9+1)-dimensional spacetime of type II string theory is factorized into a direct product of a (3+1)-dimensional external space $\mathbb{R}^{3,1}$ and a 6-dimensional internal space \mathcal{M}^6 , i.e.

$$\mathcal{X} = \mathbb{R}^{3,1} \times \mathcal{M}^6 . \quad (1.1)$$

$\mathbb{R}^{3,1}$ is the usual flat Minkowski space (also warped compact versions have been discussed) and \mathcal{M}^6 is a compact Calabi-Yau 3-fold or an orbifolded/ orientifolded T^6 , where the size of this internal manifold is small enough compared to $\mathbb{R}^{3,1}$ in order not to conflict with any gravity experiments.

Although the ansatz (1.1) seems phenomenologically obvious, it is nevertheless highly unsatisfying. If string theory is to be a fundamental theory that is valid for all energy scales, it should even be able to provide for an explanation why spacetime splits into such a product (1.1). It is more natural to assume a very isotropic and homogeneous spacetime in the very beginning of the universe, where all spatial dimensions (leaving time aside) are of the same type and size. That they should be of the same type can be concretized in the demand that they should all be either compact or non-compact. Effective compactification or decompactification of certain dimensions then could be understood dynamically within the theory. In this line of thought, a product structure (1.1) at best will be valid for late times². For this reason, it seems questionable if a model with an a priori spacetime product structure (1.1) does correctly describe early cosmology (like inflation). If inflation indeed happens at a scale $\sim 10^{10}$ GeV and the compactification scale is around the GUT scale, the ansatz (1.1) would already be sufficient to describe it.

Indeed, a picture with initially similar compact spatial dimensions has been discussed already as early as 1988 by Brandenberger and Vafa [7], where it was assumed that space in the beginning can be described by a T^9 . It is argued there that a (3+1)-dimensional large spacetime torus might be favored for late times by dimension counting arguments and considerations about Kaluza-Klein and winding modes, but these arguments were rather qualitative than quantitative.

¹which is possible if the two stacks are at a non-vanishing angle

²It is not known what ‘late times’ precisely means, as on the one hand the order of the string scale is unknown and on the other, a completely satisfying dynamical string (field) theory is missing.

We will follow a similar spirit in this paper for intersecting branes: we will not a priori require a spacetime structure (1.1), but start with a more general spacetime

$$\mathcal{X} = \text{time} \times \mathcal{M}^9, \quad (1.2)$$

where \mathcal{M}^9 is a 9-dimensional compact manifold. In order to be able to use conformal field theory methods, we will describe the simplest case, the 9-torus, $\mathcal{M}^9 = T^9$. Concretely, we will discuss the factorization

$$\mathcal{M}^9 = T^3 \times T^3 \times T^3. \quad (1.3)$$

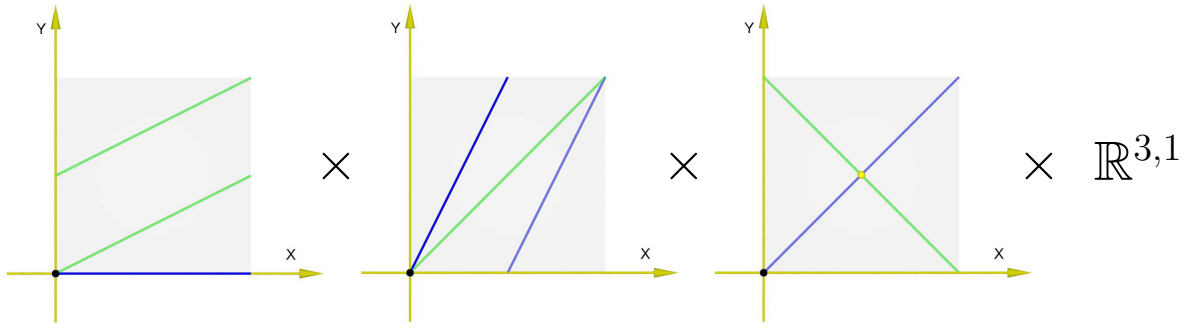
The reasons for this choice are of different nature:

1. The ansatz (1.3) seems appealing as it is the most symmetrical way for three large dimensions to emerge, i.e. one T^3 might exactly give rise to one large spatial dimension of the 4-dimensional external spacetime ($9 = 3 \times 3$).
2. The most successful models of recent years employ only D6-branes for such constructions, as they typically intersect along (3+1) common dimensions, see for instance [3, 4, 8–23]. In all the constructions, it is assumed that the D6-branes completely fill out the external space $\mathbb{R}^{3,1}$, and wrap 3-cycles on the internal space \mathcal{M}^6 that generically intersect in one (or several) point(s). The topological intersection number on the compact internal space in this case is interpreted as the multiplicity of fermion representations, or in other words, the number of generations. The string one-loop amplitude can be calculated with CFT methods exactly if the T^6 torus is factorized as $T^6 = T^2 \times T^2 \times T^2$. In this case, the 3-cycle that the D-brane wraps is factorized into three 1-cycles $\pi^{(1)}$, each wrapping one of the T^2 , i.e. $\pi^{(3)} = \pi^{(1)} \otimes \pi^{(1)} \otimes \pi^{(1)}$.

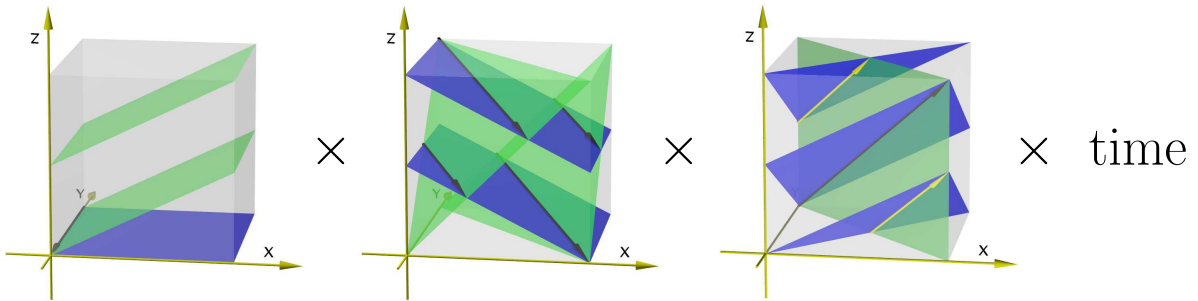
In the alternative ansatz (1.3), these computations can be generalized by simply requiring the D6-branes to wrap 2-cycles on every T^3 , i.e. $\pi^{(6)} = \pi^{(2)} \otimes \pi^{(2)} \otimes \pi^{(2)}$. The 2-cycles $\pi_a^{(2)}$ and $\pi_b^{(2)}$, describing different stacks of branes, will then generically intersect along a 1-cycle on every T^3 . This intersection 1-cycle $\pi_I^{(1)}$ is the place within each T^3 where the massless bifundamental fermions are located. The three intersection 1-cycles together (coming from the different T^3) form a 3-cycle, $\pi_I^{(3)} = \pi_I^{(1)} \otimes \pi_I^{(1)} \otimes \pi_I^{(1)}$, and together with time this is the effective 4-dimensional ‘spacetime’ for the fermion under consideration. This understanding is valid as long as the fermions are massless compared to the Planck mass. The new picture of D6-branes on the T^9 is illustrated in direct comparison to the old one on the T^6 in figure 1.

Of course, the real closed string background and therefore gravity is still (9+1)-dimensional, but this is the case as in any other brane construction in type IIA/B string theory. Such a picture can only make sense in the present state of the universe if six dimensions are small. It has been pointed out by Arkani-Hamed, Dimopoulos and Dvali in 1998 that they might be even as large as one millimeter, if only gravity is able to propagate through them [24, 25].

The wrapping of the D-branes is topological. This means that for every T^3 , the size of the intersection 1-cycle $\pi_I^{(1)}$ is dependent on the sizes of the fundamental torus



(a) The old picture on the $T^6 = T^2 \times T^2 \times T^2$



(b) The new picture on the $T^9 = T^3 \times T^3 \times T^3$

Figure 1: The two pictures of intersecting D6-branes. The total intersection number is two in both examples, meaning for (a) the number counting distinct intersection points, for (b) the number counting the distinct intersection 1-cycles (black and yellow arrows in the picture). The explicit wrapping numbers of the two branes in the lower figure are stated in table 1.

radii. If for (1.3) indeed two compactification radii within every T^3 are getting small and one is getting large, then the intersection 1-cycle $\pi_I^{(1)}$ is also getting large provided that it wraps the large torus cycle. This then implies that ‘spacetime’ for the massless fermions effectively is (3+1)-dimensional. This property is illustrated in figure 2.

3. The torus is flat. This not just allows for trustable world sheet string computations, but also agrees with the picture of cosmology of the present universe which spatially seems to be flat. This can be seen for instance in the measurements of the total energy density by the so far highest precision experiment WMAP [26], which has yielded the result $\Omega_{\text{tot}} = 1.02 \pm 0.02$, where $\Omega_{\text{tot}} = 1$ describes a flat universe within standard cosmology. Of course, this immediately poses one question: we only know that the universe is flat since the radiation of CMB, before this time the picture is not so clear. Within standard cosmology the flat universe is unstable, meaning that any initial deviation from flatness is blown up extremely during the evolution of the universe. Inflation was created particularly to solve this finetuning problem by

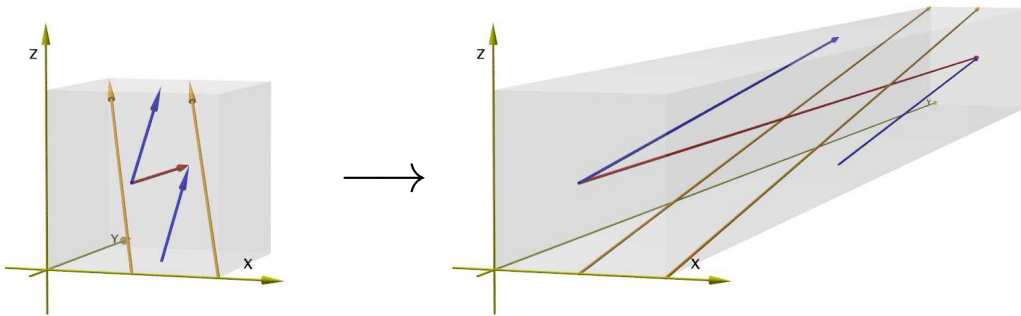


Figure 2: One radius of the T^3 growing in time. The arrows depict the intersections between different stacks of branes. Global Poincaré invariance on the left-hand-side is broken, but gets restored effectively on the right-hand-side in the late time picture.

smoothing out any initial perturbation. On the other hand, we know that standard cosmology cannot be valid for very early cosmology anyway and that string theory might replace it. This leaves the possibility that the universe could have been flat even in the very early universe and that the spatial curvature stays negligible during the evolution. This is the working hypothesis of this paper and it is possible to check the validity of this approach by calculating the backreaction of the D-branes onto spacetime explicitly.

Even if such a picture finally cannot be maintained for the whole evolution of the universe, it still can be valid for the evolution after inflation and after supersymmetry and electroweak breaking. This assumption is inherited to all non-supersymmetric intersecting brane constructions even in the context of particle physics. We know that both supersymmetry breaking and electroweak breaking surely takes place at energies above 1 TeV. Therefore, below this energy scale in the evolution of the universe, the particle spectrum should not have changed anymore and the constructed non-supersymmetric intersecting brane models should stay valid after this time.

Thus, we will discuss intersecting D6-branes that wrap general 2-cycles on every T^3 of a background (1.3). Intersecting D6-branes in type IIA string theory can be obtained from several stacks of D9-branes in type IIB with a constant but different F-flux. To see this, one has to perform three T-dualities. If we apply one T-duality in every T^3 and allow for a constant F-flux having no component in the direction in which the T-duality is performed (this is merely a technical requirement), then we indeed obtain D6-branes with vanishing F-flux. Also from this point of view, the ansatz (1.3) might be favorable. Every stack of D6-branes wraps a general 2-cycle on every T^3 being at a general angle within the T^3 . These angles are quantized in terms of three coprime wrapping numbers m' , n' and p' , as we will see later, it is completely analogue to the case on the T^2 . In this approach it is possible to construct both non-supersymmetric and supersymmetric models.

The string background $T^9 = T^3 \times T^3 \times T^3$ is not the only one that can be described exactly by CFT within this framework. This is very pleasant as D-branes alone on a compact space cannot fulfill R-R tadpole cancellation which is needed for a string model

free of gauge anomalies. The T^9 can be orientifolded and/or orbifolded, again in close analogy to the picture on the T^6 . In this paper, we will discuss the simplest case of a worldsheet Ω -orientifold in type IIB. In the type IIA picture, this translates to an ΩR -orientifold that gives rise to a geometric O6-plane. This O6-plane also wraps a geometric 2-cycle on every T^3 and R can be understood as a geometrical reflection along one of the three coordinates on every T^3 . Such a background conserves 16 supersymmetries.

1.1 Some consequences of the new picture

This picture of generally intersecting D6-branes has some interesting but unusual features which have to be addressed:

1. It is clear that all the successful models which have been constructed using the ΩR -orientifold on the $T^6 = T^2 \times T^2 \times T^2$ [11, 12] are embedded in this larger class of models, especially the prominent model with the standard model spectrum has to be mentioned [27]. In the new picture, these models are described by D6-branes that all have one common direction, such that all intersection lines are parallel on each T^3 . Subsequently, this common direction has to be decompactified. Parallel intersection 1-cycles conserve 1-dimensional Poincare invariance, therefore (3+1)-dimensional Poincare invariance is conserved. The internal space can be described by any perpendicular plane to the intersection 1-cycles in each T^3 . Every D-brane wraps a 1-cycle in this plane and these 1-cycles generically intersect along a point. One of the problems of the model [27] has been the impossibility to cancel the NS-NS tadpole. There always remains an instability in the complex structure [28, 29], implying that the brane configurations completely break supersymmetry if the tori are not degenerate. Furthermore, also the dilaton tadpole remains.
2. But in a generic model on the T^9 consisting of more than two stacks³, it might happen that the D6-branes are aligned in such a way that the intersection 1-cycles between different pairs of brane stacks are not all parallel to each other on one or several T^3 . In this case, global Poincare invariance is broken in more than six spatial directions down to (2+1)- or (1+1)-Poincare invariance, in the worst case in all of them. Nevertheless, (3+1)-Poincare invariance for just one type of particles (so for one pair of intersecting branes) by itself is always conserved. The strength of global Poincare invariance breaking surely is connected to the size proportions between the three radii within one T^3 . If one radius is very large in comparison to the others, then different intersection 1-cycles (along which distinct types of massless fermions are located) parallelize effectively. Unbroken Poincare invariance corresponds to completely parallel 1-cycles. Thus one has an effective restoration of (3+1)-dimensional Poincare invariance. It is easy to give a rough estimate that this restoration is very well off with current experimental bounds. The so-called Hughes-Drever tests⁴ so far have given the best bounds on the violation of Lorentz symmetry

³This is surely the case for the standard model which consists of three gauge factors.

⁴The deviations from the local Lorentz invariance are inferred from possible anisotropies of the inertial mass M_I in measurements of the quadrupole splitting time dependence of nuclear Zeeman levels along the orbit of the earth, $\delta = |M_I c^2 / \sum_A E^A - 1|$, where the sum goes over all forms of internal energy of a

[30], being $\delta < 3 \cdot 10^{-21}$. The diameter of the visible universe is approximately 13.7 light years. The size of the highest possible compactification scale for the small dimensions is at the millimeter scale, implying that the ratio between the largest radii and the smallest radii has to be at least $7 \cdot 10^{-30}$. This effect of Lorentz invariance restoration is illustrated in figure 2, too.

3. The same reasoning is true for supersymmetry, the D6-branes can break the initial 16 closed string supersymmetries down to any fraction or even completely. For the one-loop string amplitude, a complete breaking results in non-vanishing NS-NS tadpoles, generally in our case in one dilaton tadpole and nine radion tadpoles. It has been demonstrated that generally, NS-NS tadpoles do not indicate that the theory is inconsistent but rather that we perturb around the wrong spacetime vacuum [23, 31–35]. In order to correct this and redefine a background with vanishing NS-NS tadpole, the Fischler-Susskind mechanism (which has been invented for the dilaton tadpole in the bosonic string) should be applied [31, 32], but unfortunately there is no utilizable formulation for the NSR superstring so far. An alternative approach is to include the tadpole in the effective field theory equations of motion and then search for a new classical background [36–38]. This could allow one to really see the temporal and spatial evolution of the different closed string moduli, this would indeed be desirable for our model. But one has to be aware of the fact that this procedure only cures the problem of the tadpole in leading order (classically). Moreover, if the redefined geometry is highly curved, then the non-linear sigma model on the worldsheet cannot be solved exactly anymore.

The NS-NS tadpoles can be written as partial derivatives of a scalar potential which can be derived directly from the Born-Infeld action [39, 40], too. This scalar potential has been interpreted in the past as a dynamical potential for the scalar moduli on which it depends [28, 29, 41, 42]. This step is not trivial as the potential is actually derived for a static brane configuration, in other words, it is derived from a perturbative CFT computation which actually requires a constant spacetime background, thus one has to be careful with interpretation. Furthermore, the Born-Infeld potential includes all orders in α' , but not in the string coupling, it arises already at the open string tree-level. In the later discussion in chapter 5, we will derive also the string one-loop quantum corrections (including all orders in α'). One also has to carefully check if some bifundamental scalars during the evolution become tachyonic which is generally possible for non-supersymmetric models.

4. The most urgent question will be: can we still define our string theoretical model in a consistent way if the intersecting 1-cycles of different (3+1)-dimensional massless fermions are not always parallel on every T^3 , i.e. we globally conserve only (2+1)- or (1+1)-Poincare invariance⁵. At the level of the one-loop amplitude, this translates into the question if the R-R tadpole still can be cancelled for a general wrapping, as this would imply an anomaly free effective gauge theory. The R-R tadpole condition

chosen nucleus.

⁵The case of (0+1)-dimensional Poincare invariance breaking might be problematic in this approach due to the use of light cone gauge.

will be derived in chapter 4.1 and from the result it is indeed possible. This can be understood easily from the fact that the R-R-tadpole can be expressed purely homologically. An explicit example is discussed in detail in chapter 6.

5. In the discussed limit that all intersection 1-cycles are parallel on each T^3 , we restore the factorization of 10-dimensional spacetime (1.1) and thereby global (3+1)-dimensional Poincare invariance. The internal space can be split from the external space in a unique way for all particles simultaneously. The external space then is given by the longitudinal direction to the 1-cycles, the internal space by the transverse (orthogonal) plane. But how shall we do this splitting in the case that the intersection 1-cycles are not all parallel? To understand this, we take another look at figure 2. In the case on the left hand side, the radii all are of a similar size, a unique external 6-dimensional space cannot be defined. The picture therefore is intrinsically 10-dimensional and cannot be described by a factorization of spacetime as (1.1). Whereas if one radius is much bigger than the two other ones, like on the right hand side of figure 2, then the different transversal planes all nearly coincide with the closed string plane orthogonal to the growing radius. In the case of a complete decompactification along this growing direction, they all do exactly coincide. This leads us to the apparent conjecture that the closed string moduli actually determine the internal 6-dimensional space, and not the 1-dimensional intersections between the branes themselves. If one direction within the T^3 is very much bigger than the two orthogonal ones, then these orthogonal ones span the internal space. By the use of this plane, we can immediately get the 4-dimensional massless fermion spectrum.
6. One of the most direct effects of those solutions breaking Poincare invariance further down from (3+1) dimensions, is that Yukawa couplings obtain a small spatial dependence at the tree-level. This can be understood by the following argument: the size of the Yukawa couplings on the tree level is determined by the area of the triangle between the intersection points of the three relevant particles on the T^2 , see [43, 44]. In the new picture on the T^3 , this statement will still be valid in the plane which defines the internal space (see last point). If we move this plane along the large direction of the T^3 , then the chiral spectrum does not change (it is topological), but the distance between the particles does change. This implies that also the area of the triangle and therefore the Yukawa couplings change. In the late time picture, this locally is of course an effect which will be proportional to the ratio between the biggest and the small radii (smaller than 10^{-30} at the present state), but for the early universe it might have many new consequences which have to be considered in future work. Depending on how large the compactification scale of the large dimension compared to the visible universe actually is, there might be even visible phenomenological consequences today on a cosmological scale.
7. The first goal to see if the present construction can work is to obtain directions in the scalar moduli potential, along which certain radii grow very much compared to the other two ones on a particular T^3 . This problem is best formulated using shape and volume moduli, as will be defined in section 5.1. One shape modulus (of the two) per T^3 should have a runaway potential, the other one should be stabilized

dynamically. The overall volume of the T^9 in the late time picture should scale like the size of the present universe (an acceleration with a very small effective cosmological constant) and the relative volume ratios between the three different T^3 should have been stabilized much earlier in order to account for the isotropy of the present universe. For the very early cosmology (like before or during inflation), the picture could be very different, with many moduli not yet being stabilized. In the end it will be a very quantitative question if all of this is possible.

There are many more features of this construction which have to be thought through, we will address some of them in sections 6 and 7.

The organization of the paper is as follows. The main sections 2 to 4 deal with the precise construction of the discussed orientifold model, they are of rather technical nature and can be skipped at first reading. In section 2, we will derive the F-flux quantization of D9-branes in type IIB string theory in detail for an abelian and non-abelian flux. The results will be related to the T-dual picture of intersecting D6-branes in section 3. Also the extension to tilted 3-tori (which correspond to an additional discrete NS-NS 2-form flux) will be discussed in section 3.1. The one loop amplitude and the R-R tadpole condition will be derived in section 4.1. Subsequently, we shortly derive the supersymmetry conditions and discuss conditions for the absence of tachyons in section 4.2.

The scalar moduli potential will be discussed in section 5, including both the tree level potential in section 5.2 and the one-loop potential in section 5.3 together with a discussion of the kinetic terms in Einstein frame in section 5.1.

Finally, one concrete toy model fulfilling the R-R tadpole cancellation condition will be investigated in detail in section 6. The conclusions and prospects are stated in chapter 7.

2 Generalized magnetic flux quantization on D9-branes

At first, we will consider the simple case of just one D9-brane on a $T^9 = T^3 \times T^3 \times T^3$, carrying a $U(1)$ gauge field. Afterwards we generalize to the non-abelian $U(N)$ case of N D9-branes on top of each other.

2.1 The Abelian case

For simplicity, we define a right-handed coordinate system X_i, Y_i and Z_i on every one of the T_i^3 ($i = 1, 2, 3$). A general constant magnetic $U(1)$ flux can then be written as

$$F_{ab} = \bigotimes_{i=1,2,3} \begin{pmatrix} 0 & -B_z^i & B_y^i \\ B_z^i & 0 & -B_x^i \\ -B_y^i & B_x^i & 0 \end{pmatrix}, \quad (2.1)$$

where $a, b \in \{1, \dots, 9\}$. Of course, by a orthogonal coordinate transformation in a non-compact space we can transform this matrix into one with only one non-vanishing component of B , i.e.

$$\bigotimes_{i=1,2,3} \begin{pmatrix} 0 & -B^i & 0 \\ B^i & 0 & 0 \\ 0 & 0 & 0 \end{pmatrix}.$$

This just means that a B-field always can be represented as a vector in three dimensions and we can use a coordinate system where one coordinate axis corresponds to the direction of the B-field.

However, notice that our present case is more difficult because such a transformation has to be made simultaneously for all stacks of branes. If for different stacks the direction of the B-vector is not identical, we cannot transform the whole system of branes into a coordinate system with only one component of B . Secondly, our 3-dimensional space is compact and we cannot a priori ensure that the necessary coordinate transformation respects the lattice symmetry.

In order to be able to make a connection with the T-dual picture containing only intersecting D6-branes and vanishing B-fluxes, we will assume that there is one direction in every T^3 common to all branes, along which the B-flux is vanishing. This then will be the direction along which we perform T-duality. We make the explicit choice

$$B_z^i \equiv 0 \quad \text{for } i = 1, 2, 3. \quad (2.2)$$

This is a necessary technical requirement in order to ensure that starting from D9-branes with F-fluxes, in the D6-brane picture after T-duality there is no F-flux remaining.

In other words, we insist on a unique direction within every T^3 along which we can perform a T-duality and always get D6-branes with vanishing F-flux from the original D9-branes. If we do not make this assumption, then this might not be possible, we clearly want to avoid such a complication at this time. Choosing (2.2), it is always possible to achieve our goal by performing the T-duality in the Z_i -direction.

In the familiar case of F-fluxes on a T^6 , the flux is quantized and the constant magnetic field on the side of D9-branes can directly be related to the angle on the side of D6-branes

via the prominent equation

$$2\pi\alpha'B = \tan\varphi .$$

One expects a similar result in the generalized case of equation (2.1). This will be derived in this section. At first we will derive the flux quantization and subsequently make the connection with the branes at angles side. One has to find a vector potential A that by the equation

$$F_{ab} = \partial_a A_b - \partial_b A_a \quad (2.3)$$

reproduces the field strength (2.1) with (2.2). Such a vector potential for instance is given by the simple choice

$$A_x^i = -B_y^i Z_i, \quad A_y^i = B_x^i Z_i, \quad A_z^i = 0 . \quad (2.4)$$

The vector potential A , translated by one of the three fundamental lengths on the 3-torus, has to be gauge equivalent to the original vector potential (again for $i=1,2,3$), i.e.

$$\begin{aligned} A_x^i(X_i, Y_i, Z_i) &\sim A_x^i(X_i + 2\pi L_x^i, Y_i, Z_i) \sim A_x^i(X_i, Y_i + 2\pi L_y^i, Z_i) \sim A_x^i(X_i, Y_i, Z_i + 2\pi L_z^i), \\ A_y^i(X_i, Y_i, Z_i) &\sim A_y^i(X_i + 2\pi L_x^i, Y_i, Z_i) \sim A_y^i(X_i, Y_i + 2\pi L_y^i, Z_i) \sim A_y^i(X_i, Y_i, Z_i + 2\pi L_z^i), \\ A_z^i(X_i, Y_i, Z_i) &\sim A_z^i(X_i + 2\pi L_x^i, Y_i, Z_i) \sim A_z^i(X_i, Y_i + 2\pi L_y^i, Z_i) \sim A_z^i(X_i, Y_i, Z_i + 2\pi L_z^i). \end{aligned} \quad (2.5)$$

Therefore, a specific gauge transformation $\chi_i(X_i, Y_i, Z_i)$ has to exist that acts as an equivalence relation. For our case this requires

$$\partial_{X_i}\chi_i = -B_y^i 2\pi L_z^i, \quad \partial_{Y_i}\chi_i = B_x^i 2\pi L_z^i, \quad \partial_{Z_i}\chi_i = 0. \quad (2.6)$$

The gauge transformation then is given by

$$\chi_i = -B_y^i 2\pi L_z^i X_i + B_x^i 2\pi L_z^i Y_i + \text{const}. \quad (2.7)$$

The gauge parameter $U_i(X_i, Y_i, Z_i) \equiv \exp(i\chi_i)$ has to stay constant if one translates by any lattice vector, i.e.

$$U(X_i, Y_i, Z_i) = U(X_i + 2\pi L_x^i, Y_i, Z_i) = U(X_i, Y_i + 2\pi L_y^i, Z_i) = U(X_i, Y_i, Z_i + 2\pi L_z^i) . \quad (2.8)$$

This induces

$$\begin{aligned} \chi_i(X_i + 2\pi L_x^i, Y_i, Z_i) - \chi_i(X_i, Y_i, Z_i) &= -2\pi m_i, \\ \chi_i(X_i, Y_i + 2\pi L_y^i, Z_i) - \chi_i(X_i, Y_i, Z_i) &= 2\pi n_i, \\ \chi_i(X_i, Y_i, Z_i + 2\pi L_z^i) - \chi_i(X_i, Y_i, Z_i) &= 2\pi r_i, \end{aligned} \quad (2.9)$$

with $m_i, n_i, r_i \in \mathbb{Z}$. The fact that χ_i does not depend on Z_i forces that $r_i \equiv 0$. Writing down the first two equations explicitly using (2.7) gives us the quantization condition for the magnetic field components

$$\begin{aligned} B_x^i &= \frac{n_i}{2\pi L_y^i L_z^i} , \\ B_y^i &= \frac{m_i}{2\pi L_x^i L_z^i} . \end{aligned} \quad (2.10)$$

The 3-dimensional B -vector on every 3-torus thus is given by

$$\vec{B}_i = \frac{1}{2\pi} \begin{pmatrix} n_i/(L_y^i L_z^i) \\ m_i/(L_x^i L_z^i) \\ 0 \end{pmatrix} \quad \text{with} \quad n_i, m_i \in \mathbb{Z}. \quad (2.11)$$

It is easy to see the quantization of the flux through the three different planes spanned by two of the three fundamental T^3 coordinate axes using the definition

$$\Phi = \int_S \vec{n} \cdot \vec{B} da. \quad (2.12)$$

One simply obtains:

$$\Phi_{xy}^i = 0, \quad \Phi_{yz}^i = 2\pi n_i, \quad \Phi_{xz}^i = 2\pi m_i \quad \text{with} \quad n_i, m_i \in \mathbb{Z}. \quad (2.13)$$

2.2 The $U(N)$ case

In this section, we will generalize the result (2.10) to the non-abelian case of N D9-branes in a slightly more mathematical language using fiber bundles, an introduction to this approach can be found in [45, 46]. In order to describe a $U(N)$ bundle on a compact space (being here the direct product of three T^3), one has to chose coordinate patches on the manifold. It can be characterized by the so-called transition functions Ω_j , making the transition between different patches. In the toroidal case, one transition function per compact direction j is sufficient. These functions in general can depend on all the other compact dimensions (but not on the one for that it makes the transition), i.e. on one T^3 we have to regard

$$\Omega_1(y, z), \quad \Omega_2(x, z), \quad \Omega_3(x, y). \quad (2.14)$$

To make sure that these functions describe a well-defined bundle, they have to fulfill cocycle conditions. These ensure that for every possible path in the T^3 ending at the starting point, being described by a chain of different transitions, the result is the identity. For each T^3 one obtains three conditions (one for every pair of dimensions)

$$\begin{aligned} \Omega_1(y, 2\pi L_z) \Omega_3(0, y) \Omega_1^{-1}(y, 0) \Omega_3^{-1}(2\pi L_x, y) &= \mathbb{1} \\ \Omega_1(2\pi L_y, z) \Omega_2(0, z) \Omega_1^{-1}(0, z) \Omega_2^{-1}(2\pi L_x, z) &= \mathbb{1} \\ \Omega_2(x, 2\pi L_z) \Omega_3(x, 0) \Omega_2^{-1}(x, 0) \Omega_3^{-1}(x, 2\pi L_y) &= \mathbb{1} \end{aligned} \quad (2.15)$$

On general tori, $U(N)$ bundles are completely classified by a first Chern number per pair of dimensions, i.e. in our case

$$\begin{aligned} C_1^{xy} &\equiv \int dx dy c_1^{xy} = \frac{1}{2\pi} \int dx dy \text{Tr} \mathcal{F} = r \in \mathbb{Z}, \\ C_1^{yz} &= \frac{1}{2\pi} \int dy dz \text{Tr} \mathcal{F} = n \in \mathbb{Z}, \quad C_1^{xz} = \frac{1}{2\pi} \int dx dz \text{Tr} \mathcal{F} = m \in \mathbb{Z}. \end{aligned} \quad (2.16)$$

In this equation, \mathcal{F} stands for a general non-abelian magnetic flux. This corresponds exactly to the flux quantization condition (2.13) of the preceding section. At this point

we restrict again to $r = 0$ in order to have a good direction for performing T-duality afterwards. The gauge group $U(N)$ can be decomposed into its abelian and non-abelian components, $U(N) = (U(1) \times SU(N))/\mathbb{Z}_N$. Due to the trace which is taken in equation (2.16), only the abelian part plays an important role for the flux quantization and we obtain for the $U(1)$ part of \mathcal{F}

$$\mathcal{F}_{xy}^{U(1)} = \mathbf{0}, \quad \mathcal{F}_{yz}^{U(1)} = \frac{n}{2\pi N L_y L_z} \mathbb{1}, \quad \mathcal{F}_{xz}^{U(1)} = \frac{m}{2\pi N L_x L_z} \mathbb{1}. \quad (2.17)$$

In the following, we will see that we can indeed find concrete transition functions Ω and a connection A describing such a flux for a general choice of n and m . One set of transition functions fulfilling the cocycle conditions (2.16) is given by

$$\Omega_1 = e^{2\pi i \frac{z}{2\pi L_z} \mathbf{T}_{xz}} \mathbf{V}^m, \quad \Omega_2 = e^{2\pi i \frac{z}{2\pi L_z} \mathbf{T}_{yz}} \mathbf{V}^n, \quad \Omega_3 = \mathbb{1}, \quad (2.18)$$

where

$$\begin{aligned} \mathbf{T}_{yz} &= \text{diag} \left(\frac{n - \tilde{n}}{N}, \dots, \frac{n - \tilde{n}}{N}, \frac{n - \tilde{n}}{N} + 1, \dots, \frac{n - \tilde{n}}{N} + 1 \right), \\ \mathbf{T}_{xz} &= \text{diag} \left(\frac{m - \tilde{m}}{N}, \dots, \frac{m - \tilde{m}}{N}, \frac{m - \tilde{m}}{N} + 1, \dots, \frac{m - \tilde{m}}{N} + 1 \right), \\ \mathbf{V} &= \begin{pmatrix} 0 & 1 & & & \\ & 0 & 1 & & \\ & & 0 & \ddots & \\ & & & \ddots & 1 \\ 1 & & & & 0 \end{pmatrix}, \quad \tilde{n} \equiv n \pmod{N}, \quad \tilde{m} \equiv m \pmod{N}. \end{aligned} \quad (2.19)$$

A connection on the bundle has to fulfill the boundary conditions

$$A' = \Omega \cdot A \cdot \Omega^{-1} - i d\Omega \cdot \Omega^{-1}. \quad (2.20)$$

The prime denotes a transition along any of the three directions L_x , L_y or L_z . A constant curvature background that fulfills all the nine equations (2.20) is given by

$$\begin{aligned} A_1^0 &= A_2^0 = 0, \\ A_3^0 &= \mathcal{F}_{yz}^{U(1)} y + \mathcal{F}_{xz}^{U(1)} x + \frac{4\pi}{L_z} \text{diag} (0, 1/N, \dots, (N-1)/N) \end{aligned} \quad (2.21)$$

Therefore, the abelian part of the flux indeed is given by equation (2.17). The only important difference as compared to the purely abelian case is an additional factor N for the gauge group $U(N)$ as compared to the numerator of the two equations (2.10).

In the subsequent chapter we will see what the flux quantization in the picture of N D9-branes carrying a gauge group $U(N)$ implies for the T-dual picture of D6-branes. One technicality is still needed to understand this connection. The boundary conditions for open strings that end on the D9-brane carrying the magnetic field can be written as

$$\partial_\sigma X_a - 2\pi\alpha' F_{ab}^{U(1)} \partial_\tau X^b = 0, \quad \sigma = 0, \pi. \quad (2.22)$$

We again simplify notation by defining

$$\begin{aligned}\mathcal{B}_x &\equiv 2\pi\alpha' B_x = -2\pi\alpha' F_{yz}^{U(1)} = -\frac{\alpha'n}{NL_y L_z}, \\ \mathcal{B}_y &\equiv 2\pi\alpha' B_y = 2\pi\alpha' F_{xz}^{U(1)} = \frac{\alpha'm}{NL_x L_z}.\end{aligned}\tag{2.23}$$

For the field strength (2.17), equation (2.22) explicitly can be written as

$$\begin{aligned}\partial_\sigma X_i - \mathcal{B}_y^i \partial_\tau Z_i &= 0, \\ \partial_\sigma Y_i + \mathcal{B}_x^i \partial_\tau Z_i &= 0, \\ \partial_\sigma Z_i + \mathcal{B}_y^i \partial_\tau X_i - \mathcal{B}_x^i \partial_\tau Y_i &= 0,\end{aligned}\tag{2.24}$$

for $i = 1, 2, 3$. Passing to the worldsheet light cone derivatives defined by

$$\begin{aligned}\partial_+ &\equiv \frac{1}{2}(\partial_\tau + \partial_\sigma), \\ \partial_- &\equiv \frac{1}{2}(\partial_\tau - \partial_\sigma),\end{aligned}\tag{2.25}$$

one can rewrite the boundary conditions as follows

$$\partial_+ \begin{pmatrix} X_i \\ Y_i \\ Z_i \end{pmatrix} = \begin{pmatrix} \frac{1+\mathcal{B}_x^i - \mathcal{B}_y^i}{1+\mathcal{B}_x^i + \mathcal{B}_y^i} & \frac{2\mathcal{B}_x^i \mathcal{B}_y^i}{1+\mathcal{B}_x^i + \mathcal{B}_y^i} & \frac{2\mathcal{B}_y^i}{1+\mathcal{B}_x^i + \mathcal{B}_y^i} \\ \frac{2\mathcal{B}_x^i \mathcal{B}_y^i}{1+\mathcal{B}_x^i + \mathcal{B}_y^i} & \frac{1-\mathcal{B}_x^i + \mathcal{B}_y^i}{1+\mathcal{B}_x^i + \mathcal{B}_y^i} & \frac{-2\mathcal{B}_x^i}{1+\mathcal{B}_x^i + \mathcal{B}_y^i} \\ \frac{-2\mathcal{B}_y^i}{1+\mathcal{B}_x^i + \mathcal{B}_y^i} & \frac{2\mathcal{B}_x^i}{1+\mathcal{B}_x^i + \mathcal{B}_y^i} & \frac{1-\mathcal{B}_x^i - \mathcal{B}_y^i}{1+\mathcal{B}_x^i + \mathcal{B}_y^i} \end{pmatrix} \partial_- \begin{pmatrix} X_i \\ Y_i \\ Z_i \end{pmatrix},\tag{2.26}$$

for $i = 1, 2, 3$. This matrix will be needed in the next section for a comparison with the corresponding matrix in the T-dual picture of branes at angles.

3 Generalized intersecting D6-branes

In this chapter it is shown that a magnetic F-flux on D9-branes corresponds to T-dual D6-branes at general angles (within every T^3), if one performs a T-duality along one of the three axes of every T^3 . This is a direct generalization of the common picture of intersecting D6-branes on a T^6 .

A general rotation \mathbf{O} in three dimensions can be described by the three Euler angles, ϕ , θ and ψ , i.e. by the matrix

$$\mathbf{O} = \mathbf{BCD}\tag{3.1}$$

with the three subsequently performed rotations along the three Euler angles

$$\mathbf{B} = \begin{pmatrix} \cos \psi & \sin \psi & 0 \\ -\sin \psi & \cos \psi & 0 \\ 0 & 0 & 1 \end{pmatrix}, \quad \mathbf{C} = \begin{pmatrix} 1 & 0 & 0 \\ 0 & \cos \theta & \sin \theta \\ 0 & -\sin \theta & \cos \theta \end{pmatrix}, \quad \mathbf{D} = \begin{pmatrix} \cos \phi & \sin \phi & 0 \\ -\sin \phi & \cos \phi & 0 \\ 0 & 0 & 1 \end{pmatrix}.\tag{3.2}$$

This leads to the general rotation

$$\mathbf{O} = \begin{pmatrix} \cos \psi \cos \phi - \sin \psi \cos \theta \sin \phi & \cos \psi \sin \phi + \sin \psi \cos \theta \cos \phi & \sin \psi \sin \theta \\ -\sin \psi \cos \phi - \cos \psi \cos \theta \sin \phi & -\sin \psi \sin \phi + \cos \psi \cos \theta \cos \phi & \cos \psi \sin \theta \\ \sin \theta \sin \phi & -\sin \theta \cos \phi & \cos \theta \end{pmatrix} \quad (3.3)$$

In the frame where a D6-brane (described by a 2-cycle on every T^3) spans the two coordinate axes X'_i and Y'_i , the boundary conditions on one T^3 are simply given by two Neumann (along X'_i and Y'_i) and one Dirichlet (along Z'_i) boundary conditions, i.e.

$$\partial_+ \begin{pmatrix} X'_i \\ Y'_i \\ Z'_i \end{pmatrix} = \begin{pmatrix} 1 & 0 & 0 \\ 0 & 1 & 0 \\ 0 & 0 & -1 \end{pmatrix} \partial_- \begin{pmatrix} X'_i \\ Y'_i \\ Z'_i \end{pmatrix}. \quad (3.4)$$

If a rotation matrix \mathbf{O} takes the coordinates X_i, Y_i, \tilde{Z}_i to the primed ones,

$$\begin{pmatrix} X'_i \\ Y'_i \\ Z'_i \end{pmatrix} = \mathbf{O} \begin{pmatrix} X_i \\ Y_i \\ \tilde{Z}_i \end{pmatrix}, \quad (3.5)$$

then (3.4) can be rewritten for the unprimed coordinates and one obtains mixed Neumann/Dirichlet boundary conditions

$$\partial_+ \begin{pmatrix} X_i \\ Y_i \\ \tilde{Z}_i \end{pmatrix} = \mathbf{O}^{-1} \begin{pmatrix} 1 & 0 & 0 \\ 0 & 1 & 0 \\ 0 & 0 & -1 \end{pmatrix} \mathbf{O} \partial_- \begin{pmatrix} X_i \\ Y_i \\ \tilde{Z}_i \end{pmatrix}. \quad (3.6)$$

In order to compare with the last section, one has to include another matrix on the right hand side of this equation, taking care of the T-duality transformation on the coordinate, taking the coordinate \tilde{Z}_i into Z_i , such that the boundary conditions become

$$\partial_+ \begin{pmatrix} X_i \\ Y_i \\ Z_i \end{pmatrix} = \mathbf{O}^{-1} \begin{pmatrix} 1 & 0 & 0 \\ 0 & 1 & 0 \\ 0 & 0 & -1 \end{pmatrix} \mathbf{O} \begin{pmatrix} 1 & 0 & 0 \\ 0 & 1 & 0 \\ 0 & 0 & -1 \end{pmatrix} \partial_- \begin{pmatrix} X_i \\ Y_i \\ Z_i \end{pmatrix}. \quad (3.7)$$

Multiplying all the matrices, one obtains

$$\partial_+ \begin{pmatrix} X_i \\ Y_i \\ Z_i \end{pmatrix} = \mathbf{G} \partial_- \begin{pmatrix} X_i \\ Y_i \\ Z_i \end{pmatrix}, \quad (3.8)$$

$$\mathbf{G} \equiv \begin{pmatrix} 2 \cos^2 \theta + 2 \cos^2 \phi - 2 \cos^2 \phi \cos^2 \theta - 1 & 2 \sin \theta \sin \phi \cos \phi & 2 \sin \theta \sin \phi \cos \theta \\ 2 \sin \theta \sin \phi \cos \phi & 2 \cos^2 \phi \cos^2 \theta - 2 \cos^2 \phi + 1 & -2 \cos \theta \sin \theta \cos \phi \\ -2 \sin \theta \sin \phi \cos \theta & 2 \cos \theta \sin \theta \cos \phi & 2 \cos^2 \theta - 1 \end{pmatrix}.$$

This matrix does not depend anymore on the third angle ψ , meaning that after T-duality one obtains a 2-dimensional compact plane in every T^3 , as expected. A rotation along

ψ corresponds to one within the plane. So, the choice of Euler coordinates is indeed a very useful one. If we substitute the flux quantization (2.10) together with (2.23) into the matrix of equation (2.26), one can compare the resulting matrix element by element with \mathbf{G} . There is a one-to-one correspondence between the two matrices if one assumes that

$$\begin{aligned}\phi_i &= \arccos \left(\frac{n_i L_x^i}{\sqrt{n_i^2 L_x^i{}^2 + m_i^2 L_y^i{}^2}} \right) \\ \theta_i &= \arccos \left(\frac{L_x^i L_y^i L_z^i}{\sqrt{L_x^i{}^2 L_y^i{}^2 L_z^i{}^2 + \frac{n_i^2}{N^2} L_x^i{}^2 \alpha'^2 + \frac{m_i^2}{N^2} L_y^i{}^2 \alpha'^2}} \right)\end{aligned}\tag{3.9}$$

Now we have to rewrite the two angles for the correct lattice length in the D6-branes picture, $\tilde{L}_z^i = \alpha'/L_z^i$. Furthermore, we will rewrite the general quantum numbers n_i and m_i and also the number of D9-branes N into a combination of their coprime part n'_i , m'_i and p'_i and their greatest common divisor, $q_i \equiv \text{gcd}(n_i, m_i, N)$, such that

$$n_i = n'_i q_i \quad m_i = m'_i q_i \quad N = p'_i q_i .\tag{3.10}$$

In our approach N is positive for a D-brane, but it is also possible to formally include the case $N < 0$ and thus allow also for anti-D-branes. This statement will be made more precise later. Thereafter, we rewrite q_i for all i in the following way

$$q_i = \text{gcd}(q_1, q_2, q_3) k_i = \tilde{N} k_i \quad \text{with} \quad \tilde{N} \equiv \text{gcd}(q_1, q_2, q_3) .\tag{3.11}$$

The k_i and also N are completely fixed by the third equation in (3.10) as N does not carry any torus index, i.e.

$$k_1 = p'_2 p'_3, \quad k_2 = p'_1 p'_3, \quad k_3 = p'_1 p'_2, \quad N = p'_1 p'_2 p'_3 \tilde{N},\tag{3.12}$$

if we assume that the p'_i is a completely arbitrary integer, \tilde{N} is a positive integer. The two angles then take the new form

$$\begin{aligned}\phi_i &= \arccos \left(\frac{n'_i L_x^i}{\sqrt{n_i'^2 L_x^i{}^2 + m_i'^2 L_y^i{}^2}} \right), \\ \theta_i &= \arccos \left(\frac{p'_i L_x^i L_y^i}{\sqrt{(p'_i)^2 L_x^i{}^2 L_y^i{}^2 + n_i'^2 L_x^i{}^2 (\tilde{L}_z^i)^2 + m_i'^2 L_y^i{}^2 (\tilde{L}_z^i)^2}} \right).\end{aligned}\tag{3.13}$$

Interestingly, the positive integer \tilde{N} drops out of the two angles that now depend on nine integers n'_i , m'_i and p'_i (for the three 3-tori i). They will have a very simple geometrical interpretation as we will soon see.

First we are getting reminded of the usual case of D6-branes on the T^6 , see for instance [11]. The analogue formula for a quantized angle there is simply given by

$$\tan \phi_i = \frac{m_i L_y^i}{n_i L_x^i}$$

	m'_1	n'_1	p'_1	m'_2	n'_2	p'_2	m'_3	n'_3	p'_3
brane a (green)	-1	0	-2	-1	-1	1	1	1	0
brane b (blue)	0	0	-1	-1	0	-2	-1	1	2

Table 1: The wrapping numbers of the model shown in the lower part of figure 1.

and the two coprime integers n_i and m_i have the interpretation of wrapping numbers on a 2-torus ($i = 1, 2, 3$). A reflection at the origin of only one T , i.e. the application of the map

$$n_i \rightarrow -n_i, \quad m_i \rightarrow -m_i, \quad \text{for } i = 1, 2 \text{ or } 3,$$

has the interpretation of exchanging a brane with its corresponding anti-brane. Geometrically, it can be understood as a reversion of the orientation on one T^2 and by this also of the total orientation on the T^6 . From the sign of a certain brane contribution in the R-R-tadpole equations, one can read off that branes with a product $n_1 n_2 n_3 < 0$ are actually anti-D-branes, whereas those with $n_1 n_2 n_3 \geq 0$ correspond to D-branes. This can be seen by a comparison of this sign to that of the orientifold brane (that has a negative R-charge) within the same equation.

A similar interpretation holds in our present case: a compact two-dimensional plane within a T^3 can be uniquely specified by three integers that are mutually coprime. These integers have the interpretation of a vector in the reciprocal lattice of the T^3 , this is demonstrated in appendix A. Thus we can describe any D6-brane on one T_i^3 by a vector

$$\vec{n}_i = m'_i \mathbf{e}_1^{(i)*} + n'_i \mathbf{e}_2^{(i)*} + p'_i \mathbf{e}_3^{(i)*}, \quad (3.14)$$

where the reciprocal lattice vectors $\mathbf{e}_j^{(i)*}$ are defined by equation (A.2) in appendix A.1. Simply speaking, this vector is similar to a normal vector, with the only difference that is is defined on the reciprocal lattice and not on the lattice itself. The direction of this vector gives the orientation, reversing the orientation on one T^3 by applying the map

$$n'_i \rightarrow -n'_i, \quad m'_i \rightarrow -m'_i, \quad p'_i \rightarrow -p'_i, \quad \text{for } i = 1, 2 \text{ or } 3, \quad (3.15)$$

also here means that we make the transition from a brane to its corresponding anti-brane. Here the tadpole equation (4.20) which will be derived in section 4.1.3 reveals, that wrapping numbers $p'_1 p'_2 p'_3 \geq 0$ correspond to D-branes and wrapping numbers $p'_1 p'_2 p'_3 < 0$ to anti-D-branes.

The additional positive integer \tilde{N} on the other hand has the interpretation of the stacksize of D6-branes (or anti-D6-branes) in the type IIA picture (branes on top of each other). This can be understood by the fact that the angles do not depend on \tilde{N} but it is still present as a factor in the number of original D9-branes (the last equation in (3.12)).

The wrapping numbers of the D6-branes shown in the lower part of figure 1 are stated as an instructive example in table 1.

3.1 Introducing Tilted T^3

In the picture of D9-branes on the T^6 , it is possible to switch on an additional background NS-NS 2-form flux \mathcal{B} , such that the total magnetic flux is given by $\mathcal{B} + 2\pi\alpha'\mathcal{F}$ [47, 48].

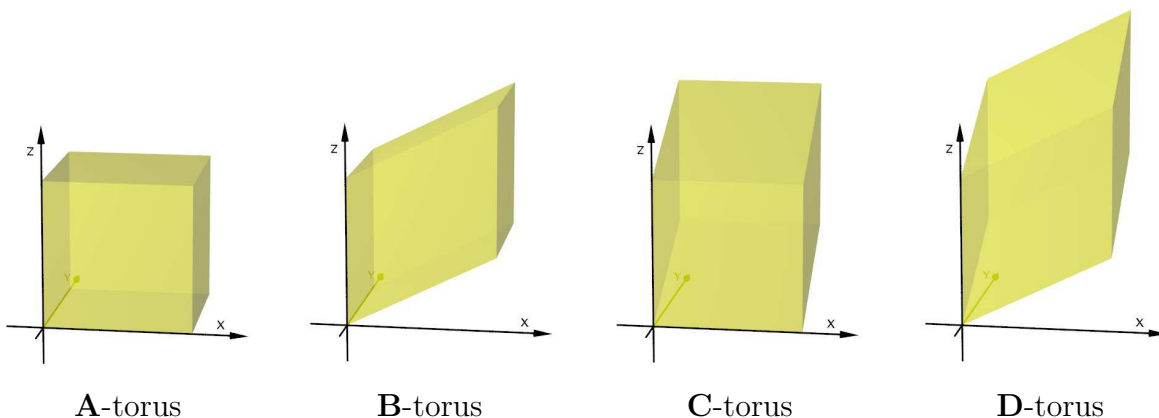


Figure 3: The four different untilted and tilted T^3 .

By applying T-duality, the \mathcal{B} -flux translates into tilted T^2 in the picture of intersecting D6-branes [12]. The \mathcal{B} -flux for the D9-branes is discrete, and on the side of branes at angles this is manifest in the fact that the geometric part of the orientifold projection ΩR allows only for certain discrete tilts of the T^2 . This is because the R projection has to map any lattice point of the torus onto another lattice point in order to respect the torus symmetry. Therefore, this fixes the angle between the two elementary radii in the type IIA picture. This fact also allows for a simple derivation of the quantization of \mathcal{B} -flux for the T^3 which will be described in the following. We assume that the tilted T^3 has a basis consisting of the three fundamental lattice vectors $2\pi L_x \mathbf{e}_1$, $2\pi L_y \mathbf{e}_2$ and $2\pi \tilde{L}_z \mathbf{e}_3$ with

$$\mathbf{e}_1 = \begin{pmatrix} c_1 \\ 0 \\ c_2 \end{pmatrix}, \quad \mathbf{e}_2 = \begin{pmatrix} 0 \\ c_3 \\ c_4 \end{pmatrix}, \quad \mathbf{e}_3 = \begin{pmatrix} 0 \\ 0 \\ c_5 \end{pmatrix}. \quad (3.16)$$

The reciprocal basis, being defined by equation (A.2), then is given by

$$\mathbf{e}_1^* = \begin{pmatrix} 1/c_1 \\ 0 \\ 0 \end{pmatrix}, \quad \mathbf{e}_2^* = \begin{pmatrix} 0 \\ 1/c_3 \\ 0 \end{pmatrix}, \quad \mathbf{e}_3^* = \begin{pmatrix} -c_2/(c_1 c_5) \\ -c_4/(c_3 c_5) \\ 1/c_5 \end{pmatrix}. \quad (3.17)$$

The reflection R reflects the X_i^* - and Y_i^* -coordinates on every T_i^3 . It maps a point of the reciprocal lattice onto another one if and only if for any $m', n', p' \in \mathbb{Z}$ three arbitrary integers $u, v, w \in \mathbb{Z}$ can be found such that the following equation holds

$$R(m' \mathbf{e}_1^* + n' \mathbf{e}_2^* + p' \mathbf{e}_3^*) = u \mathbf{e}_1^* + v \mathbf{e}_2^* + w \mathbf{e}_3^*. \quad (3.18)$$

This implies

$$u_i = -m'_i + 2p'_i \frac{L_x c_2}{\tilde{L}_z c_5}, \quad v_i = -n'_i + 2p'_i \frac{L_y c_4}{\tilde{L}_z c_5}, \quad w_i = p'_i, \quad (3.19)$$

and the right hand side of these equations will generally only be integer if

$$2 \frac{L_x c_2}{\tilde{L}_z c_5} \in \mathbb{Z}, \quad \text{and} \quad 2 \frac{L_y c_4}{\tilde{L}_z c_5} \in \mathbb{Z}.$$

We obtain four dissimilar possibilities

$$c_2 = b_1 \frac{\tilde{L}_z}{L_x} c_5, \quad c_4 = b_2 \frac{\tilde{L}_z}{L_y} c_5,$$

where $b_1, b_2 \in \{0, 1/2\}$. This result is again in direct analogy to the case on the T^6 [12]. Therefore we call the case $(b_1, b_2) = (1/2, 0)$ **B**-torus, the case $(b_1, b_2) = (0, 1/2)$ **C**-torus and the case $(b_1, b_2) = (1/2, 1/2)$ **D**-torus. The untilted torus formally is also included by $(b_1, b_2) = (0, 0)$ and will be called **A**-torus. All these possibilities are depicted in figure 3. After normalizing the lattice vectors according to $(\mathbf{e}_i)^2 = 1$, we obtain the final lattice vectors given by equations (A.4) and (A.5), as stated in appendix A.1. There will be $12 = 2 \times 6$ distinct choices for basis of the whole $T^9 = T^3 \times T^3 \times T^3$.

For simplicity in computations, it is possible to reexpress all formulae which can be derived for the tilted tori formally like for the untilted torus and vice versa [49]. In order to do so, one has to find new ‘effective’ wrapping numbers \tilde{m}' , \tilde{n}' and \tilde{p}' for the tilted torus such that R acts on them like on the untilted torus, i.e. $R(\tilde{m}'_i, \tilde{n}'_i, \tilde{p}'_i) = (-\tilde{m}'_i, -\tilde{n}'_i, \tilde{p}'_i)$. It is easy to see that this is just the case for

$$\tilde{m}'_i = m'_i + b_1 p'_i, \quad \tilde{n}'_i = n'_i + b_2 p'_i, \quad \tilde{p}'_i = p'_i. \quad (3.20)$$

To state it clearly, the orientifold projection fixes two of the three possible angles between the elementary radii to discrete values. This means that one angle (the one between the x - and the y -axis) remains unfixed. This can be seen by repeating the calculation above for two additional elements (x - and y -components) within the basis vector \mathbf{e}_3 in the ansatz 3.16. These relative size of these components is not getting fixed by the orientifold projection.

4 One-loop amplitude

In this section, we will calculate the R-R and NS-NS tadpole equations for the proposed model

$$\frac{\text{type IIA on } T^9}{\Omega R} \quad (4.1)$$

where the 9-torus is factorized as $T^9 = T^3 \times T^3 \times T^3$. This is the picture of intersecting D6-branes with a vanishing F-flux, as presented in chapter 3. We will present the computations for all T^3 being untilted, but extend the final R-R and NS-NS-tadpoles also to the case of tilted tori, as described in section 3.1.

The action of the antiholomorphic involution R will be given by

$$R: \quad \tilde{Z}_i \rightarrow -\tilde{Z}_i \quad (4.2)$$

for $i = 1, 2, 3$. This is in complete analogy to the usual orientifolds on the T^6 , where R in most cases is taken to act as a complex conjugation, also reflecting the three coordinates along which the T-duality from the D9-branes beforehand has been performed. For this simple choice (4.2), the orientifold plane is localized along the $(X_i - Y_i)$ -plane of every 3-torus.

The one-loop vacuum amplitude $\mathcal{Z}_{\text{one-loop}}$ is the sum of the 4 contributions from the different $\chi = 0$ worldsheets

$$\mathcal{Z}_{\text{one-loop}} = \mathcal{T} + \mathcal{K} + \mathcal{A} + \mathcal{M}, \quad (4.3)$$

where we will work with the Hamiltonian formalism for which every worldsheet integral is written as a trace. The torus amplitude \mathcal{T} is modular invariant and therefore finite (or even vanishing for a supersymmetric model). Hence it is irrelevant for the calculation of tadpoles and will not be treated here, only the three remaining worldsheets for which it cannot be guaranteed that they do not contain divergencies spoiling the theory at the quantum level [50, 51]. At first we will calculate the R-R-tadpole equation in the tree channel, the NS-NS tadpole is stated in appendix E.

4.1 The R-R tadpole

4.1.1 Klein bottle

The R-R sector of the tree channel Klein bottle amplitude in the loop channel corresponds to the (NS-NS, -)-sector,

$$\mathcal{K}^{(\text{NS-NS}, -)} = \sqrt{2}c \int_0^\infty \frac{dt}{t^{3/2}} \text{Tr}_{(\text{NS-NS}, -)} \left(\frac{\Omega R}{2} \frac{1 + (-1)^F}{2} e^{-2\pi t \mathcal{H}_{\text{closed}}} \right), \quad (4.4)$$

where $c = V_1 / (8\pi^2 \alpha')^{1/2}$. The trace still includes the 9-dimensional momentum integration over the compact space, whereas the integration over time already has been carried out and V_1 is its regularized length. The closed string Hamiltonian for the NS-NS loop sector is given by

$$\begin{aligned} \mathcal{H}_{\text{closed}}^{\text{NS-NS}} = & (p^\mu)^2 + \sum_\mu \left(\sum_{n=1}^\infty (\alpha_{-n}^\mu \alpha_n^\mu + \tilde{\alpha}_{-n}^\mu \tilde{\alpha}_n^\mu) \right. \\ & \left. + \sum_{r \in \mathbb{Z} + 1/2, r > 0} \left(r \psi_{-r}^\mu \psi_r^\mu + r \tilde{\psi}_{-r}^\mu \tilde{\psi}_r^\mu \right) \right) + E_0^{\text{NS-NS}} + \mathcal{H}_{\text{lattice, cl.}}^{\mathcal{K}}. \end{aligned} \quad (4.5)$$

The zero point energy in the NS-NS sector is determined by the number of complex fermions and bosons and simply given by $E_0^{\text{NS-NS}} = E_0^{\text{NS,L}} + E_0^{\text{NS,R}} = 2 \cdot 4(-1/12 - 1/24) = -1$. The lattice contribution is calculated in appendix D, equation (C.7). The trace over the oscillator modes just gives the standard NS-NS sector theta functions, altogether we obtain

$$\mathcal{K}^{(\text{NS-NS}, -)} = c \frac{\sqrt{2}}{4} \int_0^\infty \frac{dt}{t^{3/2}} \frac{-\vartheta \left[\begin{smallmatrix} 0 \\ 1/2 \end{smallmatrix} \right]^4}{\eta^{12}} \prod_{i=1}^3 \left[\sum_{s_1^i, s_2^i, r_3^i} e^{-\pi t \left(\frac{\alpha'}{L_x^i} s_1^{i2} + \frac{\alpha'}{L_y^i} s_2^{i2} + \frac{(\tilde{L}_z^i)^2}{\alpha'} r_3^{i2} \right)} \right]. \quad (4.6)$$

The argument of the ϑ and η functions is given by $q = \exp(-4\pi t)$. After the transformation into the tree channel via $t = 1/(4l)$, the Klein bottle amplitude reads

$$\tilde{\mathcal{K}}^{(\text{R-R},+)} = c \frac{16\sqrt{2}}{\alpha'^{3/2}} \int_0^\infty dl \frac{\vartheta \left[\begin{smallmatrix} 1/2 \\ 0 \end{smallmatrix} \right]^4}{\eta^{12}} \prod_{i=1}^3 \left[\frac{L_x^i L_y^i}{\tilde{L}_z^i} \left(\sum_{\tilde{s}_1^i, \tilde{s}_2^i, \tilde{r}_3^i} e^{-4\pi l \left(\frac{L_x^i{}^2}{\alpha'} (\tilde{s}_1^i)^2 + \frac{L_y^i{}^2}{\alpha'} (\tilde{s}_2^i)^2 + \frac{\alpha'}{(\tilde{L}_z^i)^2} (\tilde{r}_3^i)^2 \right)} \right) \right], \quad (4.7)$$

with an argument $q = \exp(-4\pi l)$ for the ϑ and η functions. The R-R tadpole contribution from the Klein bottle, being the zeroth order term in the q -expansion, eventually is given by

$$c \frac{256\sqrt{2}}{\alpha'^{3/2}} \prod_{i=1}^3 \left(\frac{L_x^i L_y^i}{\tilde{L}_z^i} \right). \quad (4.8)$$

4.1.2 Annulus

The (R,+)-tree channel sector corresponds to the (NS,-)-sector in the loop channel which we will now calculate. It contains four different contributions for just one stack of branes

$$\mathcal{A} = \mathcal{A}_{jj} + \mathcal{A}_{j'j'} + \mathcal{A}_{jj'} + \mathcal{A}_{j'j}. \quad (4.9)$$

The first two contributions correspond to strings going from one stack of branes to itself, whereas the third and fourth contributions represent strings that go from one brane to its mirror image, which generically is located at a non-vanishing angle. For this reason, the two types of contributions will be treated separately, we will start with the amplitude \mathcal{A}_{ii} . It is given by

$$\mathcal{A}_{jj}^{(\text{NS},-)} = c \int_0^\infty \frac{dt}{t^{3/2}} \text{Tr}_{\text{D6j-D6j}}^{(\text{NS},-)} \left(\frac{1}{2} \frac{1 + (-1)^F}{2} e^{-2\pi t \mathcal{H}_{\text{open}}^{A_{jj}}} \right). \quad (4.10)$$

The open string Hamiltonian in light cone gauge for the case of coinciding branes is given by

$$\mathcal{H}_{\text{open}}^{A_{jj}} = \frac{(p^\mu)^2}{2} + \sum_\mu \left(\sum_{n=1}^\infty (\alpha_{-n}^\mu \alpha_n^\mu) + \sum_{r \in \mathbb{Z} + \nu, r > 0} (r \psi_{-r}^\mu \psi_r^\mu) \right) + E_0 + \mathcal{H}_{\text{lattice, op.}}^{A_{jj}}, \quad (4.11)$$

The lattice contribution comprises some subtleties and is calculated in detail in appendix D.1, equation (D.21). The trace in (4.10) can be evaluated, leading to the standard theta functions in this sector from the oscillator part and a lattice sum from the Kaluza-Klein and winding contributions. After the transformation to the tree channel (see D.1 for

details), using $t = 1/(2l)$, we obtain the following amplitude for a stack of \tilde{N} branes:

$$\tilde{\mathcal{A}}_{jj}^{(R,+)} = \frac{\sqrt{2c\tilde{N}^2}}{64\alpha'^{3/2}} \int_0^\infty dl \frac{-\vartheta \begin{bmatrix} 1/2 \\ 0 \end{bmatrix}^4}{\eta^{12}} \prod_{i=1}^3 \left[\frac{n_i'^2 L_x^{i2} (\tilde{L}_z^i)^2 + m_i'^2 L_y^{i2} (\tilde{L}_z^i)^2 + p_i'^2 L_x^{i2} L_y^{i2}}{L_x^i L_y^i \tilde{L}_z^i} \sum_{w_i, k_i, l_i} e^{-2\pi l \mathcal{H}_{\text{lattice, cl.}}^{A_{jj}}} \right]. \quad (4.12)$$

The closed string lattice Hamiltonian is given in equation (D.18). The ϑ and η functions have an argument $q = \exp(-4\pi l)$. An expansion in q leads to the tadpole contribution

$$\frac{\sqrt{2c\tilde{N}^2}}{4\alpha'^{3/2}} \prod_{i=1}^3 \left[\frac{n_i'^2 L_x^{i2} (\tilde{L}_z^i)^2 + m_i'^2 L_y^{i2} (\tilde{L}_z^i)^2 + p_i'^2 L_x^{i2} L_y^{i2}}{L_x^i L_y^i \tilde{L}_z^i} \right]. \quad (4.13)$$

Next, we will calculate the annulus tadpole contributions coming from the sectors $\mathcal{A}_{jj'}$ and $\mathcal{A}_{j'j}$. These two sectors correspond to strings in between branes at a non-vanishing angle, necessitating a different treatment, also the angles appear as a summand in the moding of the oscillator sums. Nevertheless, one formally obtains exactly the same theta functions for the oscillator part as in the standard case of $T^6 = T^2 \times T^2 \times T^2$ if one simply understands the intersection angles κ_i as the angles between the normal vectors of the involved branes on the specific T^3 .

The starting equation in the loop channel then is the following

$$\mathcal{A}_{ab}^{(NS,-)} = -\frac{c}{4} \tilde{N}_a \tilde{N}_b I_{ab} \int_0^\infty \frac{dt}{t^{3/2}} e^{-\frac{3}{2}\pi t} \frac{\vartheta \begin{bmatrix} 0 \\ 1/2 \end{bmatrix} \vartheta \begin{bmatrix} \kappa_1 \\ 1/2 \end{bmatrix} \vartheta \begin{bmatrix} \kappa_2 \\ 1/2 \end{bmatrix} \vartheta \begin{bmatrix} \kappa_3 \\ 1/2 \end{bmatrix}}{\vartheta \begin{bmatrix} \kappa_1 - 1/2 \\ 1/2 \end{bmatrix} \vartheta \begin{bmatrix} \kappa_2 - 1/2 \\ 1/2 \end{bmatrix} \vartheta \begin{bmatrix} \kappa_3 - 1/2 \\ 1/2 \end{bmatrix} \eta^3} \cdot \prod_{i=1}^3 \sum_{\tilde{w}_i} e^{-2\pi t \mathcal{H}_{\text{lattice, op.}}^{A_{ab}}}. \quad (4.14)$$

The oscillator part is derived for instance in [3], but here we have an additional lattice contribution, originating from the fact, that one of the spacetime dimensions is a one-dimensional compact subset of every T^3 . κ_i is the angle between the two involved branes on the i th T^3 , the open string lattice Hamiltonian $\mathcal{H}_{\text{lattice, op.}}^{A_{ab}}$ is derived in appendix D.2, equation (D.27). I_{ab} is a multiplying factor of the amplitude which has been identified in the case of the $T^6 = T^2 \times T^2 \times T^2$ with the topological intersection number of the corresponding one-cycles of every brane on every T^2 . We will soon see that a similar meaning can be given to this factor in the case of the T^9 , there being the topological intersection number of corresponding two-cycles. But the explicit form will be more

complicated. The transformation to the tree channel leads to the following amplitude

$$\begin{aligned} \tilde{\mathcal{A}}_{ab}^{(R,+)} = & -\frac{c\sqrt{2}}{8\alpha'^{3/2}} \tilde{N}_a \tilde{N}_b I_{ab} \int_0^\infty dl \frac{\vartheta \begin{bmatrix} 1/2 \\ 0 \end{bmatrix} \vartheta \begin{bmatrix} 1/2 \\ -\kappa_1 \end{bmatrix} \vartheta \begin{bmatrix} 1/2 \\ -\kappa_2 \end{bmatrix} \vartheta \begin{bmatrix} 1/2 \\ -\kappa_3 \end{bmatrix}}{\vartheta \begin{bmatrix} 1/2 \\ 1/2 - \kappa_1 \end{bmatrix} \vartheta \begin{bmatrix} 1/2 \\ 1/2 - \kappa_2 \end{bmatrix} \vartheta \begin{bmatrix} 1/2 \\ 1/2 - \kappa_3 \end{bmatrix}} \eta^3 \\ & \cdot \prod_{i=1}^3 \left[\frac{1}{\Lambda_i} \sqrt{(p_i^{b'} n_i^{a'} - p_i^{a'} n_i^{b'})^2 L_x^2 + (m_i^{b'} p_i^{a'} - m_i^{a'} p_i^{b'})^2 L_y^2 + (m_i^{b'} n_i^{a'} - m_i^{a'} n_i^{b'})^2 (\tilde{L}_z^i)^2} \right. \\ & \left. \cdot \sum_{w_i} e^{-2\pi l \mathcal{H}_{\text{lattice, cl.}}^{A_{ab}}} \right], \quad (4.15) \end{aligned}$$

where

$$\Lambda_i \equiv \text{gcd} (m_i^{b'} p_i^{a'} - m_i^{a'} p_i^{b'}, p_i^{b'} n_i^{a'} - p_i^{a'} n_i^{b'}, m_i^{b'} n_i^{a'} - m_i^{a'} n_i^{b'}). \quad (4.16)$$

Again expanding in $q = \exp(-4\pi l)$ leads to a tadpole contribution

$$\frac{\sqrt{2}c \tilde{N}_a \tilde{N}_b I_{ab}}{4\alpha'^{3/2}} \prod_{i=1}^3 \frac{1}{\Lambda_i} \left[\frac{n_a' n_b' L_x^2 (\tilde{L}_z^i)^2 + m_b' m_b' L_y^2 (\tilde{L}_z^i)^2 + p_a' p_b' L_x^2 L_y^2}{L_x^i L_y^i \tilde{L}_z^i} \right]. \quad (4.17)$$

This expression is exactly the same contribution for the limit of coinciding branes $a = b$, equation (4.13), if one assumes that

$$I_{ab} = \prod_{i=1}^3 \Lambda_i. \quad (4.18)$$

It is indeed shown in appendix A.2 that I_{ab} is the unoriented topological intersection number between two D6-branes which correspond to 2-cycles on every T^3 . The fact that an unoriented intersection number (and not an oriented one as in the case of the T^2) appears in the amplitude is due to the fact that also the angle appearing in the theta functions is unoriented (in the sense that it is the 'smaller' angle between the two (oriented) normal vectors of the two involved branes, therefore $\leq \pi$). Further implications of this fact will be seen later.

4.1.3 R-R tadpole cancellation

We are now able to calculate the complete annulus tadpole [sum of all contributions from (4.9)] for one stack of branes, where we have to use that a ΩR -mirror brane is given by the map

$$\Omega R : \quad n_i' \rightarrow -n_i', \quad m_i' \rightarrow -m_i', \quad p_i' \rightarrow p_i'. \quad (4.19)$$

The R-R-tadpole contributions of the Klein bottle and the annulus together are sufficient to write down the full cancellation condition. Different radii factors have to cancel independently and one finally obtains the following set of tadpole cancellation conditions

(after generalizing to k stacks of branes with a stacksize \tilde{N}_l)

$$\sum_{l=1}^k \tilde{N}_l p_1^{(l)'} p_2^{(l)'} p_3^{(l)'} = 16, \quad (4.20)$$

$$\sum_{l=1}^k \tilde{N}_l p_I^{(l)'} \left(n_J^{(l)'} + b_2^J p_J^{(l)'} \right) \left(n_K^{(l)'} + b_2^K p_K^{(l)'} \right) = 0 \quad \text{with } I \neq J \neq K \neq I, \quad (4.21)$$

$$\sum_{l=1}^k \tilde{N}_l p_I^{(l)'} \left(n_J^{(l)'} + b_2^J p_J^{(l)'} \right) \left(m_K^{(l)'} + b_1^K p_K^{(l)'} \right) = 0 \quad \text{with } I \neq J \neq K \neq I, \quad (4.22)$$

$$\sum_{l=1}^k \tilde{N}_l p_I^{(l)'} \left(m_J^{(l)'} + b_1^J p_J^{(l)'} \right) \left(m_K^{(l)'} + b_1^K p_K^{(l)'} \right) = 0 \quad \text{with } I \neq J \neq K \neq I, \quad (4.23)$$

and $I, J, K \in \{1, 2, 3\}$. These equations have already been generalized to the case of tilted T^3 by introducing b_1^i and b_2^i . On every T_i^3 they independently can take the values 0 or 1/2. In general, these are $1 + 3 + 6 + 3 = 13$ different equations. Several immediate comments can be given. At first, the statement that a negative product of $p_1^{(l)'} p_2^{(l)'} p_3^{(l)'}$ corresponds to an anti-D-brane is confirmed by the first tadpole equation (4.20), as the R -charge then switches sign as compared to the O-plane that contributes the term 16 on the other side of the equation.

The tadpole equations on the standard T^6 (that have been derived in [11]) can be obtained by setting $n_J^{(l)'} = 0$ (for all l, J) and then performing the decompactification limit $L_y^i \rightarrow \infty$. Equivalently, one can set $m_J^{(l)'} = 0$ (for all l, J) and then let $L_x^i \rightarrow \infty$. In both cases, exactly four equations out of the set (4.20)-(4.23) remain and indeed are the same equations as in [11] (after renaming the wrapping numbers to the conventions used in that paper).

These equations should also be obtainable in a very different way, namely from the topological equation

$$\sum_{l=1}^k \tilde{N}_l \left(\pi^{(l)} + \pi'^{(l)} \right) - 4\pi_{O6} = 0, \quad (4.24)$$

as it has been suggested in [52], see also [27, 28]. A D6-brane which factorizes in three 2-cycles on a $T^9 = T^3 \times T^3 \times T^3$ can be written as

$$\pi^{(l)} = \pi_1^{(l)} \otimes \pi_2^{(l)} \otimes \pi_3^{(l)}, \quad (4.25)$$

where

$$\pi_i^{(l)} = p_i'^{(l)} (\pi_{x_i} \otimes \pi_{y_i}) + m_i'^{(l)} (\pi_{y_i} \otimes \pi_{z_i}) + n_i'^{(l)} (\pi_{z_i} \otimes \pi_{x_i}), \quad (4.26)$$

and i is the torus index (this case corresponds to an **AAA**-torus). The O6-plane then is located at

$$\pi_{O6} = 8 (\pi_{x_1} \otimes \pi_{y_1}) \otimes (\pi_{x_2} \otimes \pi_{y_2}) \otimes (\pi_{x_3} \otimes \pi_{y_3}) \quad (4.27)$$

and the ΩR -mirror brane can be obtained by an application of the map (4.19). One immediately obtains the set (4.20)-(4.23) for $b_1 = b_2 = 0$.

4.2 Supersymmetry conditions, absence of tachyons

The O6-brane breaks half of the supersymmetry of type IIA string theory, so in the closed string sector, there are 16 unbroken supercharges left, corresponding to $\mathcal{N} = 1$ supersymmetry in 10 dimensions. In the open string sector, the considered D6-branes in general can break this supersymmetry further down, depending on where they are located. For intersecting D-branes on the $T^6 = T^2 \times T^2 \times T^2$, several calculations have been performed in order to classify supersymmetry (see for instance [1, 53, 54]), the general result was that an angle criterion of the type

$$\phi_1 \pm \phi_2 \pm \phi_3 = 0$$

guarantees for some unbroken supersymmetry. ϕ_i is the oriented angle between two stacks of D6-branes on the i th 2-torus, where one of the stacks preserves half of the type IIA closed string supersymmetry. In an orientifold background, the angle criterion still holds if we understand the angles as those in between the O6-plane and a certain stack of D-branes on every 2-torus. This condition then can be interpreted as a calibration condition, requiring that both the special Lagrangian cycles (that the D-branes wrap) and the orientifold brane are calibrated with respect to $\Re(\Omega_3)$, where Ω_3 is a holomorphic 3-form [52].

Following the worldsheet approach of [53], it is possible to characterize spacetime supersymmetry in an elegant way by just looking at the one-loop annulus amplitudes between different branes. Some supersymmetry is conserved when the NS and corresponding R amplitudes of that particular sector exactly cancel against each other, i.e.

$$\tilde{\mathcal{A}}_{ab}^{(R,+)} - \left(\tilde{\mathcal{A}}_{ab}^{(NS,+)} + \tilde{\mathcal{A}}_{ab}^{(NS,-)} \right) = 0. \quad (4.28)$$

The amplitude $\tilde{\mathcal{A}}_{ab}^{(R,+)}$ is explicitly given in equation (4.15), the corresponding NS-amplitude only differs by the theta equations in the numerator of the first fraction (for a detailed discussion see [3]). Therefore, one immediately obtains the following supersymmetry condition

$$\begin{aligned} \vartheta \begin{bmatrix} 1/2 \\ 0 \end{bmatrix} \vartheta \begin{bmatrix} 1/2 \\ -\kappa_1 \end{bmatrix} \vartheta \begin{bmatrix} 1/2 \\ -\kappa_2 \end{bmatrix} \vartheta \begin{bmatrix} 1/2 \\ -\kappa_3 \end{bmatrix} - \vartheta \begin{bmatrix} 0 \\ 0 \end{bmatrix} \vartheta \begin{bmatrix} 0 \\ -\kappa_1 \end{bmatrix} \vartheta \begin{bmatrix} 0 \\ -\kappa_2 \end{bmatrix} \vartheta \begin{bmatrix} 0 \\ -\kappa_3 \end{bmatrix} \\ + \vartheta \begin{bmatrix} 0 \\ 1/2 \end{bmatrix} \vartheta \begin{bmatrix} 0 \\ 1/2 - \kappa_1 \end{bmatrix} \vartheta \begin{bmatrix} 0 \\ 1/2 - \kappa_2 \end{bmatrix} \vartheta \begin{bmatrix} 0 \\ 1/2 - \kappa_3 \end{bmatrix} = 0, \end{aligned} \quad (4.29)$$

where κ_i is the smaller angle ($< \pi$) between the normal vectors between one stack of branes a and another one b on the i th 3-torus, as explained earlier. Expanding the theta functions in q leads to the leading contribution equation

$$\cos^2(\kappa_1) + \cos^2(\kappa_2) + \cos^2(\kappa_3) - 2 \cos(\kappa_1) \cos(\kappa_2) \cos(\kappa_3) = 1. \quad (4.30)$$

The possible solutions to this equation are given by

$$\kappa_1 \pm \kappa_2 \pm \kappa_3 = 0 \quad (4.31)$$

This angle criterion at first sight coincides with the angle criterion on the T^6 . Again the case of an orientifold background can formally be included in this analysis by taking the angles κ to be those between the orientifold plane normal vector and the D-brane⁶.

But there is one very important subtlety as compared to the case on the T^6 : the angles are lying in a three-dimensional space. The overall annulus amplitude for several stacks of branes will only vanish (and therefore the whole system will be supersymmetric), if all possible annulus amplitude sectors between different branes and between different branes and the O6-plane vanish separately. In the case of the T^6 it is guaranteed that overall SUSY is preserved if every one of the branes is aligned supersymmetrically to the O6-plane. If for two different D6-branes the angle criterion is fulfilled separately (with the angle taken in between the D-brane and the O-plane), i.e.

$$\phi_1^a + \phi_2^a + \phi_3^a = 0, \quad \phi_1^b + \phi_2^b + \phi_3^b = 0,$$

then these two D-branes are also aligned supersymmetrically against each other,

$$(\phi_1^a - \phi_1^b) + (\phi_2^a - \phi_1^b) + (\phi_3^a - \phi_1^b) = 0,$$

simply because the rotations on every 2-torus are commutative and are performed in the same 2-plane (being the T^2 itself). This is not the case for the $T^9 = T^3 \times T^3 \times T^3$, equation (4.31), as these angles are taken in between 3-dimensional vectors and therefore do not necessarily lie within the same 2-plane. Consequently, we really have to require (4.31) for all different possible sectors between all stacks of branes and in addition between all these stacks and the O-plane in order to conserve some supersymmetry. It is possible to count the conserved supersymmetries by looking at the potential bifundamental scalars⁷ in the NS-sector in between two stacks of branes [14, 27]. Their masses are controlled by the angles between the branes, in our case those that appear in equation (4.31). Their masses are given by

$$\begin{aligned} \alpha' M_1^2 &= \frac{1}{2} (-\kappa_1 + \kappa_2 + \kappa_3), & \alpha' M_2^2 &= \frac{1}{2} (\kappa_1 - \kappa_2 + \kappa_3), \\ \alpha' M_3^2 &= \frac{1}{2} (\kappa_1 + \kappa_2 - \kappa_3), & \alpha' M_4^2 &= 1 - \frac{1}{2} (\kappa_1 + \kappa_2 + \kappa_3). \end{aligned} \quad (4.32)$$

For a supersymmetric configuration fulfilling the angle criterion (4.31), some of these four equations will be zero, the remaining ones positive and this lets us directly determine the amount of unbroken supersymmetry. For a non-supersymmetric configuration, it might happen that some of these masses become negative and thus tachyonic. This signals an instability and according to [55] on a Calabi-Yau can be interpreted in a way that the joining process of the branes is energetically favored. There are attempts to understand these tachyons as Higgs field in the effective theory (see for instance [28, 42] and references within), but the validity of this approach seems rather questionable as it is an off-mass-shell process. The point of view taken in this article is to avoid tachyons if possible. It carefully has to be checked for any explicit model, if this is indeed possible⁸. We will

⁶although there is no annulus amplitude of this kind, as the orientifold brane itself only contributes to the Klein-bottle and Möbius amplitudes. On the other hand our formal treatment is equivalent to calculating the annulus amplitudes between a brane and its ΩR mirror image, $\tilde{A}_{jj'}$.

⁷if they are really there depends on the topological intersection number I_{ab} between the branes under consideration.

⁸Note that the angles vary with a change of the torus radii.

come back to this question in the explicit example in section 6.

5 The scalar potential

The (perturbative) scalar potential for the moduli is contained in the perturbative vacuum partition function. The open string partition function contains all diagrams of a certain world sheet topology, weighted with a factor of the open string coupling constant, $\exp(-\chi\tilde{\phi}_0^{(10)})$. In this factor, χ is the Euler number, $\chi = 2 - 2g - b - c$ and $\tilde{\phi}_0^{(10)}$ is the expectation value of the 10-dimensional dilaton within type IIA string theory⁹. The lowest contributing open string diagrams are the disc and the projective plane, which both have an Euler number one and will be called open string tree level diagrams. The open string next to leading order diagrams are the annulus (cylinder) and Möbius strip diagrams which have an Euler number zero, they will be called open string one loop diagrams. We can schematically write down the open string vacuum partition function as

$$\mathcal{Z} = e^{-\tilde{\phi}_0^{(10)}} (\text{disc} + \text{projective plane}) + e^0 (\mathcal{A} + \mathcal{M}) + \text{higher loop contributions.} \quad (5.1)$$

The scalar potential for the moduli then can also be written as

$$V_{\text{scalar}} = V_{\text{tree}} + V_{\text{1-loop}} + \text{higher loop contributions,} \quad (5.2)$$

and every scalar potential contribution arises from the corresponding partition function contribution. The tree-level potential can be derived from the Born Infeld potential in type IIB (and a similar reasoning is true for the orientifold plane). Alternatively, the disc and projective plane diagrams can be normalized from the one-loop partition function. The one-loop potential has to be calculated within the worldsheet approach.

Both potentials give contributions that are independent of α' , but also α' corrections. The latter ones are specific to string theory and might play an important role for the understanding of the discussed model as we will see.

There are two further subtleties that one has to take into account in order to speak about the physical meaning of the scalar potential within our universe: the potential has to be transformed into the Einstein frame. After this procedure, one can simplify the physical picture in two more ways. Instead of the radii, one can equally well switch to shape and volume moduli (similar to the imaginary part of the complex and Kaehler structures in the T^2). Furthermore, for convenience, one can make a field redefinition into new scalar variables with canonically normalized kinetic terms as in common field theory.

All these procedures require a very careful treatment of the prefactors of the different potential contributions, including both powers of α' and the dilaton expectation value, in order to judge their relative importance. Therefore, we will discuss the relevant kinetic terms in the following subsection.

One technical problem arises if α' corrections indeed play an important role. In this case it is hard to get an understanding of the spacetime picture, because also higher derivative kinetic terms most likely have to be taken into account in the Einstein frame in order to integrate the equations of motion, which is generally not well understood up till now. We will come back to this point later.

⁹A similar result holds in type IIB.

5.1 The kinetic terms in effective field theory

We are interested in the kinetic terms of the metric components and the dilaton. All these closed string scalar moduli are contained in the NS-sector of type IIA string theory, for which the effective action can be written as [56]

$$S_{\text{NS}} = \frac{1}{2\kappa_{10}^2} \int d^{10}x \sqrt{-G} e^{-2\tilde{\phi}_{10}} [\mathcal{R}_{10} + 4 \partial_\mu \phi_{10} \partial^\mu \phi_{10} + \mathcal{O}(\alpha')] , \quad (5.3)$$

where we have assumed that $H_3 \equiv 0$. Writing the torus metric in the diagonal form¹⁰ and assuming only a time dependence,

$$G_{\mu\nu} = \text{diag} \left(-g_{00}(t), L_x^1(t)^2, L_y^1(t)^2, \tilde{L}_z^1(t)^2, L_x^2(t)^2, L_y^2(t)^2, \tilde{L}_z^2(t)^2, L_x^3(t)^2, L_y^3(t)^2, \tilde{L}_z^3(t)^2 \right), \quad (5.4)$$

one can write the action as an one-dimensional one. The 10-dimensional dilaton has to be dimensionally reduced to the one dimensional one by using

$$e^{-\tilde{\phi}^{(10)}} = \frac{e^{-\tilde{\phi}^{(1)}} \alpha^{9/4}}{\prod_{i=1}^3 \sqrt{L_x^i L_y^i \tilde{L}_z^i}}. \quad (5.5)$$

Subsequently, we can go into the 1-dimensional Einstein frame. In order to do so, we first define the dilaton $\phi_{\text{E}}^{(1)}$ with a vanishing expectation value,

$$\phi_{\text{E}}^{(1)}(t) = \tilde{\phi}^{(1)}(t) - \tilde{\phi}_0^{(1)}, \quad (5.6)$$

and then rescale the metric by

$$G_{\mu\nu}^{\text{E}} = e^{-\frac{4}{D-2}\phi_{\text{E}}^{(D)}(t)} G_{\mu\nu} = e^{4\phi_{\text{E}}^{(1)}(t)} G_{\mu\nu}. \quad (5.7)$$

This leads to the effective action [after assuming $g_{00}(t) \equiv 1$ in (5.4)] for the kinetic terms

$$S_{\text{NS}}^{\text{E}} = \frac{16\pi^2 \alpha'^{1/2}}{e^{2\tilde{\phi}_0^{(1)}}} \int dt \left[\sum_{i=1}^9 \left(-\frac{1}{2} \left(\frac{\dot{L}_{\text{E}}^i}{L_{\text{E}}^i} \right)^2 + 9 \frac{\dot{L}_{\text{E}}^i}{L_{\text{E}}^i} \dot{\phi}_{\text{E}}^{(1)} \right) - \frac{1}{2} \sum_{i=1}^9 \sum_{j>i} \left(\frac{\dot{L}_{\text{E}}^i \dot{L}_{\text{E}}^j}{L_{\text{E}}^i L_{\text{E}}^j} \right) - 73 \left(\dot{\phi}_{\text{E}}^{(1)} \right)^2 + \frac{1}{4} e^{-4\phi_{\text{E}}^{(1)}} \mathcal{O}(\alpha') \right], \quad (5.8)$$

where the dots denote the derivative with respect to t . The term $9\ddot{\phi}_{\text{E}}^{(1)}$ does not play any role for the equations of motion (as it is a surface term) and has been omitted. For convenience of writing, the different torus radii in the metric have been renamed from 1 to 9. We will later factor out the same prefactors for the action of the tree-level and one-loop potential.

Later we will see that it is very useful to reformulate both potentials in terms of volume and (dimensionless) shape moduli of the T^3 in order to get a better physical understanding. Such a procedure is analogous to the change of variables from the radii to complex

¹⁰This is the case for the case where all b_1^i and b_2^i are identically zero.

structure and Kähler moduli in case of the T^2 , their imaginary parts corresponding to shape and volume moduli. We thus define the following moduli for each T_i^3 :

$$q_{xz}^i = \frac{L_{x,E}^i}{\tilde{L}_{z,E}^i}, \quad q_{yz}^i = \frac{L_{y,E}^i}{\tilde{L}_{z,E}^i}, \quad V_{\text{tot}} = V_E^1 V_E^2 V_E^3, \quad V_{13} = \frac{V_E^1}{V_E^3}, \quad V_{23} = \frac{V_E^2}{V_E^3}, \quad (5.9)$$

where $V_E^i = L_{x,E}^i L_{y,E}^i \tilde{L}_{z,E}^i$ is the volume of the i th 3-torus, q_{xz} is the shape parameter in the (x,z) - and q_{yz} in the (y,z) -plane, this is for the specific T^3 with orthogonal axes.

Instead of the original 9 radii moduli, we now have 6 shape moduli q_{xz}^i and q_{yz}^i (which describe the ratios between two tori axes on each T_i^3), the overall T^9 volume V_{tot} and the two ratios between the volume of two of the T_i^3 , V_{13} and V_{23} . This new choice will prove to be very useful for a better physical understanding, as will be seen in the subsequent sections. The kinetic terms (5.8) take a simpler form in terms of these new moduli:

$$\begin{aligned} S_{\text{NS}}^E = & \frac{16\pi^2 \alpha'^{1/2}}{e^{2\tilde{\phi}_0^{(1)}}} \int dt \left(\sum_{i=1}^9 \left[-\frac{1}{6} \left(\frac{\dot{q}_{xz}^i}{q_{xz}^i} \right)^2 - \frac{1}{6} \left(\frac{\dot{q}_{yz}^i}{q_{yz}^i} \right)^2 + \frac{1}{6} \frac{\dot{q}_{xz}^i \dot{q}_{yz}^i}{q_{xz}^i q_{yz}^i} \right] - \frac{5}{18} \left(\frac{\dot{V}_{\text{tot}}}{V_{\text{tot}}} \right)^2 \right. \\ & \left. - \frac{1}{18} \left(\frac{\dot{V}_{13}}{V_{13}} \right)^2 - \frac{1}{18} \left(\frac{\dot{V}_{23}}{V_{23}} \right)^2 + \frac{1}{18} \left(\frac{\dot{V}_{13} \dot{V}_{23}}{V_{13} V_{23}} \right) - 73 \left(\dot{\phi}_E^{(1)} \right)^2 + 9 \frac{\dot{V}_{\text{tot}}}{V_{\text{tot}}} \dot{\phi}_E^{(1)} + \frac{1}{4} e^{-4\phi_E^{(1)}} \mathcal{O}(\alpha') \right). \end{aligned} \quad (5.10)$$

The contributions of the shape moduli can be separated into terms for the three different T_i^3 , no mixing occurs between different tori. Additionally, there are simple kinetic terms for the overall volume and the volume ratios. The dilaton mixes only with the overall volume, and the two volume ratios mix with one another. In order to get canonically normalized kinetic terms, one can make field redefinitions,

$$\begin{aligned} \tilde{V}_{\text{tot}} &= \sqrt{\frac{5}{9}} \ln V_{\text{tot}}, & \tilde{V}_{13} &= \frac{1}{3} \ln V_{13}, & \tilde{V}_{23} &= \frac{1}{3} \ln V_{23}, \\ \tilde{q}_{xz}^i &= \sqrt{\frac{1}{3}} \ln q_{xz}^i, & \tilde{q}_{yz}^i &= \sqrt{\frac{1}{3}} \ln q_{yz}^i, & \phi_c^{(1)} &= \sqrt{146} \phi_E^{(1)}, \end{aligned} \quad (5.11)$$

such that the standard kinetic terms get the canonical form, but the mixing terms of course still occur and not all of them have canonical prefactors.

5.2 The tree-level potential

The Born-Infeld action of type IIB string theory for N_l coinciding D9-brane(s) with a constant $U(1)$ or $U(N_l)$ flux, as discussed in sections 2.1 and 2.2, respectively, in general is given by

$$\mathcal{S}_{\text{DBI}} = T_9 \int_{D9_l} d^{10}x e^{-\phi^{(10)}} \sqrt{\det \left(G_{\mu\nu} + 2\pi\alpha' F_{\mu\nu}^{(l)} \right)}, \quad (5.12)$$

where T_p stands for the Dp-brane tension

$$T_p = \frac{\sqrt{\pi}}{\kappa_{(10)}} (4\pi^2 \alpha')^{\frac{3-p}{2}} \quad (5.13)$$

and $\kappa_{(10)}^2 = 1/2(2\pi)^7\alpha'^4$. Therefore, the tension has a dependence $T_9 \sim \alpha'^{-5}$ and the action is dimensionless.

By inserting the metric $G_{\mu\nu} = \delta_{\mu\nu}$ and the F-flux (2.23) for all three T^3 into this equation, we obtain the square root of the determinant

$$\sqrt{\det\left(G_{\mu\nu} + 2\pi\alpha'F_{\mu\nu}^{(l)}\right)} = \prod_{i=1}^3 \sqrt{1 + \frac{\alpha'^2 n_i^2}{N_l^2 L_y^2 L_z^2} + \frac{\alpha'^2 m_i^2}{N_l^2 L_x^2 L_z^2}}. \quad (5.14)$$

We can now integrate over the 9-dimensional compact space, where we assume that the 10-dimensional dilaton is spatially constant, as is the F-flux. This implies also that the compactification radii L_i are assumed to be spatially constant (they do not depend on each other).

One has to take into account that N_l D9-branes wrap the 9-dimensional torus together N_l times, and that this in the picture of the T-dual D6-branes can be written as $N_l = p'_1 p'_2 p'_3 \tilde{N}_l$, according to the last equation in (3.12). We also rewrite the other quantum numbers using (3.10). Furthermore, we have to rewrite the three radii into the T-dual type IIA ones, $\tilde{L}_z^i = \alpha'/L_z^i$, and rewrite the dilaton in the T-dual picture,

$$e^{-\phi^{(10)}} = \frac{\tilde{L}_z^1 \tilde{L}_z^2 \tilde{L}_z^3}{\alpha'^{3/2}} e^{-\tilde{\phi}^{(10)}}, \quad (5.15)$$

and then rewrite the tension using

$$T_9 = \frac{T_6}{(2\pi\sqrt{\alpha'})^3}. \quad (5.16)$$

One finally obtains

$$\mathcal{S}_{\text{DBI}} = T_6 (2\pi)^6 \tilde{N}_l \int dt e^{-\tilde{\phi}^{(10)}} \prod_{i=1}^3 \sqrt{n_i'^2 L_x^i{}^2 (\tilde{L}_z^i)^2 + m_i'^2 L_y^i{}^2 (\tilde{L}_z^i)^2 + p_i'^2 L_x^i{}^2 L_y^i{}^2}, \quad (5.17)$$

As all the spatial dimensions are compact and integrated out, one can equally well dimensionally reduce the dilaton to only the dimension of time using equation (5.5) and then write (5.17) as

$$\mathcal{S}_{\text{DBI}} = T_6 (2\pi)^6 \alpha'^{9/4} \tilde{N}_l \int dt e^{-\tilde{\phi}^{(1)}} \prod_{i=1}^3 \sqrt{n_i'^2 \frac{L_x^i \tilde{L}_z^i}{L_y^i} + m_i'^2 \frac{L_y^i \tilde{L}_z^i}{L_x^i} + p_i'^2 \frac{L_x^i L_y^i}{\tilde{L}_z^i}}. \quad (5.18)$$

This expression can be understood as the tree level scalar potential for one stack of \tilde{N}_l D6-branes [14, 28, 29, 42], i.e. $\mathcal{S}_{\text{DBI}} = \int dt V_{\text{tree}}[\tilde{\phi}^{(1)}(t), L_x^i(t), L_y^i(t), \tilde{L}_z^i(t)]$.¹¹ Together with the ΩR mirror branes and the orientifold plane, one obtains the following total scalar

¹¹If one does not want to understand the potential as a time dependent one, one can just integrate time formally out and thus write an additional factor $(2\pi V_1)$ in front, where V_1 is the regularized time.

potential in the string frame

$$\mathcal{S}_{\text{DBI}} = \int dt 2T_6 (2\pi)^6 \alpha'^{9/4} e^{-\tilde{\phi}^{(1)}} \cdot \left[\sum_{l=1}^k \tilde{N}_l \prod_{i=1}^3 \sqrt{\left(n_i^{(l)'} + b_2^i p_i^{(l)'} \right)^2 \frac{L_x^i \tilde{L}_z^i}{L_y^i} + \left(m_i^{(l)'} + b_1^i p_i^{(l)'} \right)^2 \frac{L_y^i \tilde{L}_z^i}{L_x^i} + p_i^{(l)'}{}^2 \frac{L_x^i L_y^i}{\tilde{L}_z^i}} - 16 \prod_{i=1}^3 \sqrt{\frac{L_x^i L_y^i}{\tilde{L}_z^i}} \right]. \quad (5.19)$$

We have extended this equation to the case of tilted T^3 by including b_1^i and b_2^i , $b_1^i, b_2^i \in \{0, 1/2\}$, corresponding to an additional discrete B-flux in the Born-Infeld potential (5.12) as discussed in section 3.1. In the limit $n_i^{(l)'} = 0$ (for all l, i) and subsequently, $L_y^i \rightarrow \infty$, this potential does exactly agree with the one derived in [28, 29] for the $T^6 = T^2 \times T^2 \times T^2$. One only has to rewrite the 1-dimensional dilaton in terms of the 4-dimensional one (taking into account that in this limit the three L_y^i are the three additional spatial dimensions of 4-dimensional spacetime). This is unproblematic as these dimensions have been integrated out in both cases (T^3 and T^2).

Going to the 1-dimensional Einstein frame by using equations (5.6) and (5.7), the tree level potential finally takes the form

$$\mathcal{S}_{\text{DBI}}^{\text{E}} = \frac{16\pi^2 \alpha'^{1/2}}{e^{2\tilde{\phi}_0^{(1)}}} \int dt V_{\text{tree}}^{\text{E}}, \quad (5.20)$$

where

$$V_{\text{tree}}^{\text{E}} = \frac{e^{\tilde{\phi}_0^{(1)}}}{8\alpha'^{7/4}\pi^2} e^{-4\phi_{\text{E}}^{(1)}} \cdot \left[\sum_{l=1}^k \tilde{N}_l \prod_{i=1}^3 \sqrt{\left(n_i^{(l)'} + b_2^i p_i^{(l)'} \right)^2 \frac{L_{x,\text{E}}^i \tilde{L}_{z,\text{E}}^i}{L_{y,\text{E}}^i} + \left(m_i^{(l)'} + b_1^i p_i^{(l)'} \right)^2 \frac{L_{y,\text{E}}^i \tilde{L}_{z,\text{E}}^i}{L_{x,\text{E}}^i} + p_i^{(l)'}{}^2 \frac{L_{x,\text{E}}^i L_{y,\text{E}}^i}{\tilde{L}_{z,\text{E}}^i}} - 16 \prod_{i=1}^3 \sqrt{\frac{L_{x,\text{E}}^i L_{y,\text{E}}^i}{\tilde{L}_{z,\text{E}}^i}} \right]. \quad (5.21)$$

It is most instructive to rewrite the tree-level potential in terms of the shape and volume moduli, defined by (5.9). The result for all twists $b_1^i = b_2^i = 0$ is given by

$$V_{\text{tree}}^{\text{E}} = \frac{e^{\tilde{\phi}_0^{(1)}}}{8\alpha'^{7/4}\pi^2} e^{-4\phi_{\text{E}}^{(1)}} V_{\text{tot}}^{1/6} \cdot \left[\sum_{l=1}^k \tilde{N}_l \prod_{i=1}^3 (q_{xz}^i q_{yz}^i)^{1/3} \sqrt{\frac{n_i^{(l)'}{}^2}{q_{yz}^i} + \frac{m_i^{(l)'}{}^2}{q_{xz}^i} + p_i^{(l)'}{}^2} - 16 \prod_{i=1}^3 (q_{xz}^i q_{yz}^i)^{1/3} \right]. \quad (5.22)$$

Some important remarks regarding this potential have to be given:

1. The tree level potential depends only on the total T^9 volume V_{tot} in a way $\sim V_{\text{tot}}^{1/6}$, but it does not depend on the volume ratios between the different T_i^3 . In terms of the canonical variables (5.11), this implies a dependence $\sim \exp[1/\sqrt{60}\tilde{V}_{\text{tot}}]$. In terms of the volumes of the different T_i^3 , they all trivially have a similar potential $\sim V_E^{i/6}$. This behavior is independent of the wrapping numbers and thus general. Disregarding the kinetic terms, the overall volume (and at the same time the volume of every T_i^3) cannot be stabilized, it tends to zero.
2. The dependence of the potential on the time-dependent one-dimensional dilaton is $\sim \exp[-4\phi_E^{(1)}]$, this is again a general statement. The dilaton shows a runaway behavior on the tree-level.
3. This is different for the shape moduli q_{xz}^i and q_{yz}^i . Depending on the wrapping numbers of the different stacks of branes, the behavior of every stack contribution can be either $\sim (q^i)^{1/3}$ or $\sim (q^i)^{-2/3}$. For the canonical variables, this translates into a behavior $\sim \exp[\frac{1}{\sqrt{3}}\tilde{q}^i]$ or $\sim \exp[-\frac{2}{\sqrt{3}}\tilde{q}^i]$. In the interplay between different stack contributions and the orientifold plane, it is even possible to stabilize some of the q^i on the tree-level. This can be seen for instance in the explicit example of section 6.

5.3 The one-loop potential

As explained in the introduction of this chapter, the one-loop potential contribution arises from the annulus and Möbius partition functions of the worldsheet calculation. If there is a NS-NS tadpole, these amplitudes then formally are diverging due to the lowest (zeroth) order contribution in the modular function expansion parameter $q = \exp(-4\pi l)$. This divergence is simply the NS-NS tadpole itself. In [42] the suggestion has been made to regularize every diagram simply by subtracting the NS-NS tadpole, indeed this seems to make sense as the higher orders in q do not lead to any additional divergence. Therefore, this somewhat crude procedure will be used here, too.

For a given number k of stacks of D6-branes, the complete annulus amplitude is given by

$$\begin{aligned} \tilde{\mathcal{A}}_{\text{tot}} = & \sum_{l=1}^k \left(\tilde{\mathcal{A}}_{ll} + \tilde{\mathcal{A}}_{l'l'} + \tilde{\mathcal{A}}_{ll'} + \tilde{\mathcal{A}}_{l'l} \right) \\ & + \sum_{l < j} \left(\tilde{\mathcal{A}}_{lj} + \tilde{\mathcal{A}}_{jl} + \tilde{\mathcal{A}}_{l'j'} + \tilde{\mathcal{A}}_{j'l'} + \tilde{\mathcal{A}}_{lj'} + \tilde{\mathcal{A}}_{j'l} + \tilde{\mathcal{A}}_{l'j} + \tilde{\mathcal{A}}_{j'l} \right) . \end{aligned} \quad (5.23)$$

and every amplitude can be directly obtained from the two general formulas in the R-sector (4.15) and 4.12). The additional NS-sector amplitudes only differ in the usual way in the arguments of the ϑ -functions. The complete Möbius amplitude consists of the contributions

$$\tilde{\mathcal{M}}_{\text{tot}} = \sum_{l=1}^k \left(\tilde{\mathcal{M}}_l + \tilde{\mathcal{M}}_{l'} \right) , \quad (5.24)$$

and every contribution can be obtained already from the Klein-Bottle and annulus amplitudes, this is for instance explained in [3]. The regularization can be done independently for every term. In order to compare with the result at the tree-level, one again has to transform into the 1-dimensional Einstein frame and write the potential as a time-dependent one. This will be done exemplary in the remainder of this section for an amplitude of the type $\tilde{\mathcal{A}}_{ab}$. From Jacobi's abstruse identity,

$$\vartheta^4 \begin{bmatrix} 0 \\ 0 \end{bmatrix} (q) - \vartheta^4 \begin{bmatrix} 0 \\ 1/2 \end{bmatrix} (q) - \vartheta^4 \begin{bmatrix} 1/2 \\ 0 \end{bmatrix} (q) = 0, \quad (5.25)$$

it follows that the amplitude vanishes when brane a and brane b coincide, i.e. for all three angles $\kappa_i \equiv 0$. This is surely the case for $\tilde{\mathcal{A}}_{ll}$ and $\tilde{\mathcal{A}}_{l'l'}$ in the total annulus amplitude (5.23), but can be the case for even more contributions. All non-vanishing contributions therefore have at least one non-vanishing angle κ_i on any T_i^3 . Exemplary, we will discuss the specific case where $\kappa_1 \neq 0$ and $\kappa_2 \neq 0$, but $\kappa_3 = 0$ in the remainder of this section. In Einstein frame, the potential takes the following form:

$$\tilde{\mathcal{A}}_{ab}^{\text{reg,E}} = \frac{16\pi^2 \alpha'^{1/2}}{e^{2\tilde{\phi}_0^{(1)}}} \int dt V_{1\text{-loop}}^{ab,\text{E}}, \quad (5.26)$$

where

$$\begin{aligned} V_{1\text{-loop}}^{ab,\text{E}} &= e^{2\tilde{\phi}_0^{(1)} - 6\phi_{\text{E}}^{(1)}} \frac{\tilde{N}_a \tilde{N}_b}{512\pi^3 \alpha'^{5/2}} \cdot \frac{n_3'^2 (L_{x,\text{E}}^3)^2 (\tilde{L}_{z,\text{E}}^3)^2 + m_3'^2 (L_{y,\text{E}}^3)^2 (\tilde{L}_{z,\text{E}}^3)^2 + p_3'^2 (L_{x,\text{E}}^3)^2 (L_{y,\text{E}}^3)^2}{L_{x,\text{E}}^3 L_{y,\text{E}}^3 \tilde{L}_{z,\text{E}}^3} \\ &\cdot \prod_{i=1}^2 \left[\sqrt{(p_i^{b'} n_i^{a'} - p_i^{a'} n_i^{b'})^2 (L_{x,\text{E}}^i)^2 + (m_i^{b'} p_i^{a'} - m_i^{a'} p_i^{b'})^2 (L_{y,\text{E}}^i)^2 + (n_i^{b'} n_i^{a'} - m_i^{a'} n_i^{b'})^2 (\tilde{L}_{z,\text{E}}^i)^2} \right] \\ &\cdot \int_0^\infty dl \left[\left(\frac{-\vartheta^2 \begin{bmatrix} \frac{1}{2} \\ 0 \end{bmatrix} \vartheta \begin{bmatrix} \frac{1}{2} \\ -\kappa_1 \end{bmatrix} \vartheta \begin{bmatrix} \frac{1}{2} \\ -\kappa_2 \end{bmatrix}}{\vartheta \begin{bmatrix} \frac{1}{2} \\ \frac{1}{2} - \kappa_1 \end{bmatrix} \vartheta \begin{bmatrix} \frac{1}{2} \\ \frac{1}{2} - \kappa_2 \end{bmatrix}} \eta^6 \right. \right. \\ &\quad \left. \left. + \frac{\vartheta^2 \begin{bmatrix} 0 \\ 0 \end{bmatrix} \vartheta \begin{bmatrix} 0 \\ -\kappa_1 \end{bmatrix} \vartheta \begin{bmatrix} 0 \\ -\kappa_2 \end{bmatrix} - \vartheta^2 \begin{bmatrix} 0 \\ \frac{1}{2} \end{bmatrix} \vartheta \begin{bmatrix} 0 \\ \frac{1}{2} - \kappa_1 \end{bmatrix} \vartheta \begin{bmatrix} 0 \\ \frac{1}{2} - \kappa_2 \end{bmatrix}}{\vartheta \begin{bmatrix} \frac{1}{2} \\ \frac{1}{2} - \kappa_1 \end{bmatrix} \vartheta \begin{bmatrix} \frac{1}{2} \\ \frac{1}{2} - \kappa_2 \end{bmatrix}} \eta^6 \right) \\ &\cdot \left(\sum_{w_1} e^{-2\pi l \mathcal{H}_{\text{lat, cl.}, T_1^3}^{A_{ab},\text{E}}} \right) \left(\sum_{w_2} e^{-2\pi l \mathcal{H}_{\text{lat, cl.}, T_2^3}^{A_{ab},\text{E}}} \right) \left(\sum_{w_3, k_3, l_3} e^{-2\pi l \mathcal{H}_{\text{lat, cl.}, T_3^3}^{A_{jj},\text{E}}} \right) - 1 \right]. \quad (5.27) \end{aligned}$$

The Einstein frame lattice Hamiltonians on the first two T^3 are of the form

$$\begin{aligned} \mathcal{H}_{\text{lat, cl.}, T_i^3}^{A_{ab},\text{E}} &= \frac{e^{-4\phi_{\text{E}}^{(1)}}}{2\alpha' \Lambda_i^2} \left[(p_i^{b'} n_i^{a'} - p_i^{a'} n_i^{b'})^2 (L_{x,\text{E}}^i)^2 + (m_i^{b'} p_i^{a'} - m_i^{a'} p_i^{b'})^2 (L_{y,\text{E}}^i)^2 \right. \\ &\quad \left. + (n_i^{b'} n_i^{a'} - m_i^{a'} n_i^{b'})^2 (\tilde{L}_{z,\text{E}}^i)^2 \right] w_i^2 \quad \text{for } i = 1, 2, \quad (5.28) \end{aligned}$$

and the one on the third torus is of the form

$$\begin{aligned}
\mathcal{H}_{\text{lat, cl., } T_3^3}^{A_{jj,E}} &= \frac{e^{4\phi_E^{(1)}} \alpha'}{2} \left[\frac{m_3'^2}{(L_{x,E}^3)^2} + \frac{n_3'^2}{(L_{y,E}^3)^2} + \frac{p_3'^2}{(\tilde{L}_{z,E}^3)^2} \right] w_3^2 \\
&+ \frac{e^{-4\phi_E^{(1)}}}{2\alpha'} \left[\left(\frac{n_3'^2}{d_3^2} (L_{x,E}^3)^2 + \frac{m_3'^2}{d_3^2} (L_{y,E}^3)^2 \right) k_3^2 + \left(\frac{n_3' p_3' x_3}{d_3} (L_{x,E}^3)^2 - \frac{m_3' p_3' y_3}{d_3} (L_{y,E}^3)^2 \right) 2k_3 l_3 \right. \\
&\quad \left. + \left(p_3'^2 x_3^2 (L_{x,E}^3)^2 + p_3'^2 y_3^2 (L_{y,E}^3)^2 + d_3^2 (\tilde{L}_{z,E}^3)^2 \right) l_3^2 \right]. \quad (5.29)
\end{aligned}$$

The symbols Λ_i , d_i , x_i and y_i are some number-theoretical constants (depending on the actual wrapping numbers) and are defined in appendices D.1 and D.2. Beware that the symbol t in equation (5.26) denotes time (and not the loop channel modular parameter) but l denotes the tree-channel modular parameter. Interestingly, the actual angles κ_i (and therefore the ϑ -functions) do not depend on the Einstein-rescaling of the metric as they are dimensionless. The subtracted 1 in (5.27) is due to the regularization scheme. A general analysis of the one-loop potential contribution (5.27) is much more difficult. One has to perform a modular integration over l and within the integral there is a product of modular ϑ and η -functions times the product of five infinite sums. The fraction containing the ϑ - and η -functions can be q -expanded as stated in appendix F, equation (F.1), and different orders can be integrated over l separately (after the multiplication with the Kaluza-Klein and winding sums). Due to the complicated structure of the Hamiltonians, the Kaluza-Klein and winding summation later in the example will be performed only for a finite number of summation terms. For each term, the integration over l then is performed analytically.

It is instructive to reformulate both the 1-loop potential (5.27) and the two Hamiltonians (5.28) and (5.29) in terms of the shape, overall volume and volume ratio moduli, as defined in equation (5.9). The following general observations can be made:

1. The angles κ_i do neither depend on the dilaton, the overall volume or the volume ratios, only on the shape moduli. Together with the terms in front of the modular integral, this leads to a dilaton dependence $\sim \exp[-6\phi_E^{(1)}]$. The remaining modular integral can be performed for every term of the infinite sum separately. The structure of every single term before integration is of the form

$$\sim \exp[-2\pi l(h_1 w_1^2 + h_2 w_2^2 + h_3 w_3^2 + h_4 k_3^2 + h_5 l_3^2)]$$

Every h_i has a dependence on the dilaton of either $\sim \exp[-4\phi_E^{(1)}]$ or $\sim \exp[4\phi_E^{(1)}]$. After the integration has been performed (over all but the constant divergent term which has been subtracted), the leading order terms for large $\phi_E^{(1)}$ have a behavior $\sim \exp[4\phi_E^{(1)}]$. Together with the terms in front, this implies that the overall behavior of the one loop potential (from the annulus amplitude) is at best $\sim \exp[-2\phi_E^{(1)}]$, so the run-away behavior of the dilaton cannot be cured at the one-loop level.

2. A similar reasoning can be performed for the overall volume modulus V_{tot} . The dependence of all terms in front of the modular integral together is $\sim V_{\text{tot}}^{1/3}$. Every

stacksize	m'_1	n'_1	p'_1	m'_2	n'_2	p'_2	m'_3	n'_3	p'_3
$N_a=4$	0	0	1	0	1	1	1	0	4
$N_b=2$	-1	-1	-1	0	1	0	1	-1	0
$N_c=1$	3	0	2	0	1	0	-1	-1	0

Table 2: The wrapping numbers of the three stack model on the **AAA**-torus discussed in the text.

h_i in the Hamiltonian of the infinite sums has a dependence of either $\sim V_{\text{tot}}^{2/9}$ or $\sim V_{\text{tot}}^{-2/9}$. After the integration, the leading order behavior (for large V_{tot}) is $\sim V_{\text{tot}}^{2/9}$ for these terms and the overall behavior of the potential is $\sim V_{\text{tot}}^{5/9}$. Thus the overall volume tends to shrink to zero also at the one-loop level (ignoring kinetic terms). One seems to need non-perturbative effects of fluxes in order to change this behavior.

3. The behavior of the other moduli is very much dependent on the actual wrapping numbers of a model and is much more promising as will be seen for the explicit example in the following section.

6 An explicit example

The most important consistency condition for any explicit string theoretical model containing intersecting branes is the R-R tadpole condition. It has been derived explicitly in terms of wrapping numbers in section 4.1 and is stated in equations (4.20)-(4.23). The crucial question now is if there are models containing more than two stacks of branes, where the intersection between different stacks are not all parallel on a specific T^3 . As such models globally break Poincare invariance down to (2+1) or (1+1) dimensions, it would most likely contain new features as compared to the old picture on the T^6 (where (3+1)-dimensional Poincare invariance is conserved for all times by definition).

It is much more involved to give a systematic analysis on all R-R charge cancelling models in the new framework, simply because there are nine instead of six wrapping numbers for every stack¹². Especially for extensions of the well-known standard model of [27] this is problematic as it employs at least $l = 4$ stacks. The purpose of this section is not to give one specific completely satisfying model already, but simply to get an understanding of the general picture, some more detailed explicit constructions will follow in the future [57]. The model which is presented here is a toy model.

A computer program was set up in order to search for such a 3-stack toy model which fulfills the R-R tadpole cancellation condition on the most simple **AAA**-torus. One completely arbitrary model that has been found is stated explicitly in table 2. It fulfills the R-R tadpole condition and the intersections between the different stacks are not all parallel on the first and third T^3 , but they are on the second torus. This implies that total Poincare invariance is broken down to (1+1)-dimensions. Supersymmetry is not

¹²If we only take into account all integer wrapping numbers from -3 up till 3, this in total implies 7^{l-9} different possibilities, compared to 7^{l-6} on the T^6 , where l denotes the number of stacks.

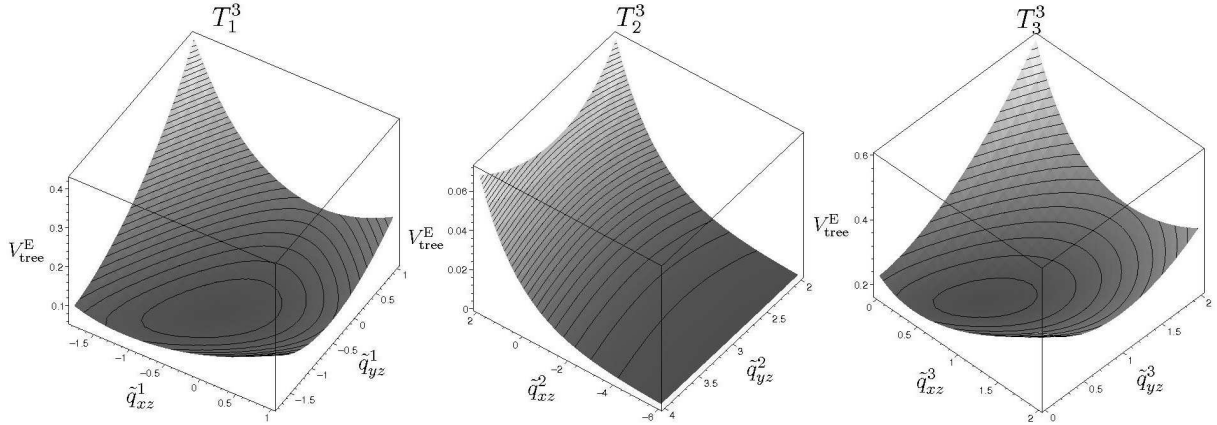


Figure 4: Complete tree-level scalar potential dependence on canonically normalized shape moduli for the explicit example. The plots are shown on each T_i^3 separately, with the other shape moduli fixed.

conserved, and the next step is to discuss the complete scalar potential in Einstein frame, starting with the tree-level potential.

The overall volume dependence of the tree-level potential is generally $\sim V_{\text{tot}}^{1/6}$, and the dilaton dependence is $\sim \exp[-4\phi_E^{(1)}]$. There is no dependence on the volume ratio moduli V_{13} and V_{23} between the different T_i^3 , meaning that (if kinetic terms play no crucial role), all three T_i^3 change volume uniformly.

In order to be able to plot the potential for the remaining moduli, we therefore fix both dilaton and overall volume terms identically to one. Furthermore, we will fix both the string coupling $e^{\tilde{\phi}_0^{(1)}}$ and α' identically to one, the latter meaning that we measure all dimensionful scales in terms of the string length. The total tree-level potential then (containing the different terms from all stacks and the orientifold plane) is shown in figure 4 for the canonical variables (5.11). For any of the three plots (corresponding to one of the different T_i^3), the shape moduli of the other two T_i^3 have been fixed to one. This ignores the interaction between the different T_i^3 , but seems to be a good approximation locally close to the string length. This is underlined by the fact that there are no kinetic mixing terms between the shape moduli of the different T_i^3 , see equation (5.10).

It can be seen on the plots that a different kind of behavior is possible on the three T_i^3 , depending completely on the particular chosen wrapping numbers on that torus. On the first T_1^3 and the third T_3^3 , the potential has indeed a minimum in which both shape moduli q_{xz}^i and q_{yz}^i (for $i=1,3$) can be stabilized. These local minima can be verified by partially differentiating the potential (5.22). They are lying at the numerical values ($q_{xz}^1 \approx 0.520$, $q_{yz}^1 \approx 0.249$) and ($q_{xz}^3 \approx 3.539$, $q_{yz}^3 \approx 2.767$) (note that in the figure the canonically normalized variables have been plotted). The situation is different on the second T_2^3 . There is no local minimum for both shape moduli q_{xz}^2 and q_{yz}^2 at the same time. (which also can be checked numerically by differentiation). In particular, the modulus q_{xz}^2 has no local minimum, but the modulus q_{yz}^2 has one if we hold q_{xz}^2 constant. The reason for this behavior is easy to see looking at the wrapping numbers: $m'_2 = 0$ for all stacks of branes. No brane wraps around this cycle in the reciprocal lattice. This

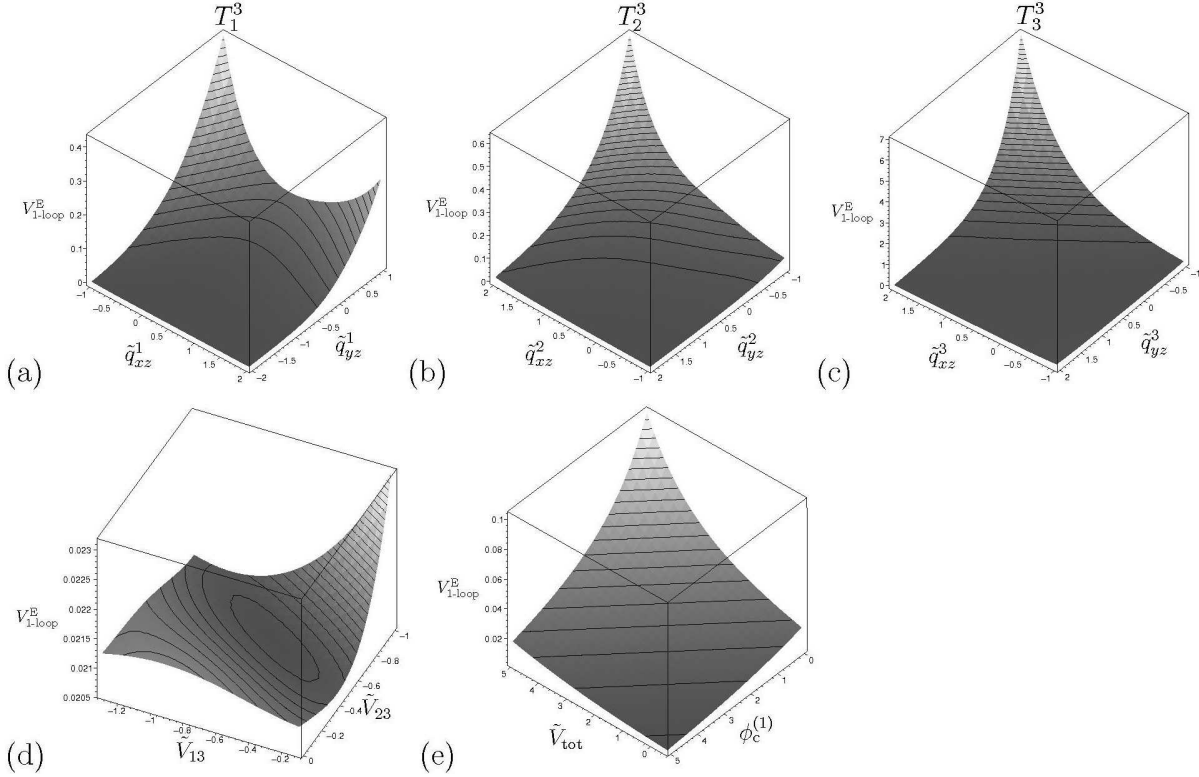


Figure 5: One-loop scalar potential dependence on canonically normalized moduli for the explicit example from annulus amplitude \mathcal{A}_{bc} . The moduli not occurring in a certain plot are fixed.

implies that the intersections between all branes on the second T_2^3 stretch parallel in the L_x^2 -direction, so this is the common space-time direction on that torus. According to the second plot in 4, the radius L_x^2 shrinks compared to the other two. This is a very interesting and general result, as it means that by wrapping all cycles on a certain T^3 , we at least stabilize the ratios between the three radii at the tree-level, such that no radius shrinks to zero compared to the other two ones, this happens in the common picture that the T^3 can be factorized into $T^3 = T^2 \times T^1$. This is of course not yet enough, as we would actually like one radius to grow and the other two to be stabilized compared to each other at a constant scale. In other words, we would like to have one q to be growing appropriately and the other one to be stabilized. This might still happen at the one-loop level, so we now take a look at the one-loop potential.

The potential from the annulus amplitude $\hat{\mathcal{A}}_{bc}$ is calculated exemplarily, it is exactly of the form as treated in chapter 5.3. But at the same time, we have to be aware that it only gives a part of the whole picture and that the sum of all amplitudes might still change it even qualitatively (especially as we disregard the first stack of branes). Nevertheless, we will surely gain some understanding. The one loop potential is calculated numerically, after an analytical integration of the modular integral over l . The constant part in the expansion of the ϑ - and η - functions is folded with the five series, for those only the terms from -1 up to 1 are being taken into account. The NS-NS tadpole which is the

only divergent term in the integral is getting subtracted for regularization. The resulting potential is plotted in figure 5 for several pairs of the scalar moduli varying, with the others fixed. All the fixed moduli in every plot are taken equal to one (besides the dilaton which is taken to be $\exp[\phi_E^{(1)}] = 1$) and also $\exp[\tilde{\phi}_0^{(1)}]$ and α' are set to one. Some comments immediately can be given:

1. Plot (e) in figure 5 shows the potential dependence of the one-dimensional dilaton and the overall volume which has been anticipated generally already in the end of section 5.3. The dilaton still has a runaway potential which is at least decaying as $\sim \exp[-2\phi_E^{(1)}]$, the overall volume dependence is decaying at least as $\sim V_{\text{tot}}^{5/9}$ (the plot shows the canonically normalized variables).
2. Plot (d) shows the two volume ratio moduli \tilde{V}_{13} and \tilde{V}_{23} (which measure the relative ratio of each two of the T^3 volumes). These two moduli have a flat potential on the tree-level and it seems that at the one-loop level they can be stabilized even at a local minimum. This is a very nice feature, because it means that all three tori grow (or decay) in size simultaneously, none of them changes size with a different scaling from the other two. This seems to be a requirement for the observed isotropy of the visual universe.
3. Plot (a)-(c) show the two shape moduli of every T_i^3 in relation to each other. The results are quite different from those at the tree level. On the first torus, figure (a), one modulus is being stabilized and the other one runs towards zero size. At the tree level, both generically are being stabilized (it was guessed that this is the general behavior if all cycles on the T_i^3 are being wrapped by some brane). So at the one-loop level, for one modulus this behavior is changed. An even more interesting behavior occurs on the second and third torus, figures (b) and (c), one modulus is being stabilized at zero size, the other one in all likelihood shows a runaway behavior. This is the behavior we actually wanted from the start, as it means that one radius grows in size compared to the other two and these are stabilized compared to each other. It is of course far from being obvious that this solves our problem, as the relative importance of tree-level and one-loop potential depends on many different things, mainly on both the vacuum expectation value of the dilaton and the time-dependent Einstein frame dilaton. Nevertheless, it is very encouraging to see that the scaling behavior of the potential dependence on the time-dependent dilaton can be different for tree-level and one-loop potential. A direct comparison between the general dilaton dependence on the tree-level and the numerically calculated dependence on the one-loop level (for the given example) shows that for a larger overall volume, the one-loop contributions can grow in importance compared to the tree-level contributions. It is of course an intricate task to show that the string perturbation series then still can converge. It can be guessed that a working mechanism of this kind will require some fine-tuning.

7 Conclusions and prospects

In this paper, the general formalism to describe D6-branes on a orientifolded background $T^3 \times T^3 \times T^3$ has been developed, where the D-branes are allowed to wrap general 2-cycles on every T^3 . The one-loop partition function has been derived and the R-R tadpole equations have been calculated. As expected, the result for the R-R tadpole is homological and depends only on the stack sizes and the nine topological wrapping numbers of every stack of branes. This determines the chiral massless fermion spectrum.

The complete scalar moduli potential on the tree-level has been derived. The general results are that the 1-dimensional Einstein frame dilaton has a runaway potential $\sim \exp[-4\phi_E^{(1)}]$ and that the overall T^9 volume dependence is $\sim V_{\text{tot}}^{1/6}$. The two ratios V_{13} and V_{23} between the relative volumes of the 3-tori do not receive a potential contribution at this level. The picture for the six shape moduli q_{xz}^i and q_{yz}^i ($i=1,2,3$) depends on the actual wrapping numbers and stack sizes of all D-branes. It seems that they can be stabilized if some D-brane wraps around the corresponding elementary cycle. If no D-brane wraps around certain cycles (as is the case for the old known (3+1)-dimensional Poincare invariant solutions in this new framework), the corresponding shape moduli shrink to zero size.

Also the one-loop potential from the annulus amplitudes is derived in a general form, where the modular integration still has to be performed. This makes it technically rather difficult to obtain general (not model dependent) results for a complicated brane configuration. The general results are that the 1-dimensional dilaton in Einstein frame still has a runaway potential and that the overall volume still shrinks to zero. On the other hand, V_{13} and V_{23} are typically stabilized at the one-loop. This is of course a very important feature, as it assures anisotropy of the three large spatial directions of the universe at late times (provided that the rest of the proposed mechanism works). Furthermore, the shape moduli can actually run off to infinity, run to zero or even stay stabilized (as on the tree level), this is completely dependent on the actual wrapping numbers.

So far only annulus amplitudes were considered, but it is well possible that the Möbius amplitude (involving the orientifold planes) can give opposite sign contributions to the potential and this could alter the general picture. One can also think about other possibilities to stabilize the dilaton and to alter the overall volume dependence, the two being the two most important problems of the present construction. They could be solved for example by taking into account non-perturbative effects or by adding fluxes. It could also be that kinetic terms play an important role in the evolution, but this most probably requires the potential for the overall volume to be very flat.

Then it will be necessary to think more quantitatively about the shape moduli. How large do the wrapping numbers have to be in order to describe such an enormous size difference between the different radii as by a factor 10^{30} ? It is interesting to note that in the explicitly discussed model, the relative minima where the shape moduli are stabilized at the tree-level are directly related to the wrapping numbers. The canonically normalized shape moduli are on a logarithmic scale, this suggests that a difference of 60 e -foldings (as described by inflation) could only need wrapping numbers of a size like 60. Then the next question would be, if it is possible to get phenomenologically interesting spectra (like that of the standard model) for the same wrapping numbers in the late time picture? From

experience this seems very well possible, see for instance [28]. The global evolution of the universe would be intimately related to the massless fermion spectrum in a single model, this surely would make such a model much more falsifiable (or verifiable) and bring string theory closer to its original goal of describing very different energy scales at the same time. The technical tools are there, but the enormous number of potential models makes it rather difficult to handle.

A general T^3 has six moduli, as shown in appendix B, of which in the present ansatz only five are present, the three radii and two angles which are fixed by the orientifold projection to discrete values. It will be interesting to extend this formalism in the future to include also the additional angle modulus. Another future step could be to see if orbifolding the T^3 could cure some of the present problems as on the T^2 , see for instance [21,28,58]. Naively, one just has to make the transition from the five 2-dimensional Bravais lattices to the fourteen 3-dimensional ones. This could also bring $N = 1$ supersymmetry back into the game (supersymmetric configurations could be limiting cases that the system dynamically evolves to).

To go even further, other more general 3-manifolds could be considered as a possible background, but this surely would require extraordinary technical expenses.

There is even the possibility that the general philosophy proposed in this paper even allows for a quantization of the moduli space itself in a simple setting (like the $T^3 \times T^3 \times T^3$), instead of just constructing string theory on this classical background. But this surely is an even farther reaching goal.

Acknowledgments

I would like to thank S. Bruers, M. Billo, A. Keurentjes and L. Martucci for helpful and lengthy discussions. Then the very helpful advices and also the interest from the mathematician Joost van Hamel and furthermore Wouter Castryck and Hendrik Hubrechts have to be mentioned with best thanks. Further nice discussions include R. Blumenhagen, A. Krause, A. Miemiec, I. Kirsch, I. Runkel, A. Celi, F. Passerini, J. Adam, G. Smet, P. Smyth, J. Van den Bergh, D. Van den Bleeken, W. Troost, L. Görlich, L. Huiszoon and A. Sen. For proofreading of the article I would like to thank J. Rosseel and A. van Proeyen and at the same time B. Körs for helpful comments on an earlier stage of the manuscript.

This work is supported in part by the European Community's Human Potential Programme under contract MRTN-CT-2004-005104 'Constituents, fundamental forces and symmetries of the universe'. The work of T.O. is supported in part by the FWO - Vlaanderen, project G.0235.05 and by the Federal Office for Scientific, Technical and Cultural Affairs through the "Interuniversity Attraction Poles Programme – Belgian Science Policy" P5/27.

A Topology of 2-cycles on the T^3

At the beginning of this section, we will show in a very simple way that a 2-cycle on a T^3 , being characterized by the two angles ϕ and θ from equation (3.13) can be uniquely described by a primitive vector in the reciprocal lattice of the 3-torus, eq. (A.2). The two

angles include three quantum numbers n' , m' and p' that are coprime. A 2-dimensional cycle that spans the (x, y) -plane of the T^3 trivially can be described by a perpendicular vector along the z direction. Two orientations are possible. We assign to the plane facing 'upwards' the vector $(0, 0, 1/L_z)$. If we now apply the rotation matrix \mathbf{O} from (3.3) together with (3.13) on this vector, the resulting vector is proportional to

$$\vec{n} \equiv \left(\frac{m'}{2\pi L_x}, \frac{n'}{2\pi L_y}, \frac{p'}{2\pi \tilde{L}_z} \right). \quad (\text{A.1})$$

This is a general primitive vector in the reciprocal lattice, because n' , m' and p' are arbitrary coprime integers. Consequently, there is a one-to-one correspondence between primitive vectors in the reciprocal lattice of T^3 and possible 2-cycles in the lattice of T^3 .

A.1 Lattice definitions

Every T^3 has the three fundamental cycles $2\pi L_x \mathbf{e}_1$, $2\pi L_y \mathbf{e}_2$ and $2\pi \tilde{L}_z \mathbf{e}_3$, where the lattice vectors \mathbf{e}_i are normalized to $(\mathbf{e}_i)^2 = 1$. The reciprocal lattice is defined by

$$\mathbf{e}_i \mathbf{e}_j^* = \delta_{ij}, \quad (\text{A.2})$$

where the basis takes the form $1/(2\pi L_x) \mathbf{e}_1^*$, $1/(2\pi L_y) \mathbf{e}_2^*$ and $1/(2\pi \tilde{L}_z) \mathbf{e}_3^*$.

A.1.1 The A-torus

The **A**-torus can be defined by the following lattice vectors

$$\mathbf{e}_1 = \mathbf{e}_1^* = \begin{pmatrix} 1 \\ 0 \\ 0 \end{pmatrix}, \quad \mathbf{e}_2 = \mathbf{e}_2^* = \begin{pmatrix} 0 \\ 1 \\ 0 \end{pmatrix}, \quad \mathbf{e}_3 = \mathbf{e}_3^* = \begin{pmatrix} 0 \\ 0 \\ 1 \end{pmatrix}. \quad (\text{A.3})$$

The lattice and reciprocal lattice vectors can be chosen to take the same form in this type of torus, as the axes are all perpendicular. The reciprocal lattice vectors \mathbf{e}_i^* therefore are also normalized to $(\mathbf{e}_i^*)^2 = 1$.

A.1.2 The B, C and D-tori

The other three discussed tori can be defined by the following lattice vectors

$$\mathbf{e}_1 = \begin{pmatrix} \sqrt{1 - \left(b_1 \frac{\tilde{L}_z}{L_x}\right)^2} \\ 0 \\ b_1 \frac{\tilde{L}_z}{L_x} \end{pmatrix}, \quad \mathbf{e}_2 = \begin{pmatrix} 0 \\ \sqrt{1 - \left(b_2 \frac{\tilde{L}_z}{L_y}\right)^2} \\ b_2 \frac{\tilde{L}_z}{L_y} \end{pmatrix}, \quad \mathbf{e}_3 = \begin{pmatrix} 0 \\ 0 \\ 1 \end{pmatrix}. \quad (\text{A.4})$$

They lead to the following reciprocal lattice vectors

$$\mathbf{e}_1^* = \begin{pmatrix} 1/\sqrt{1 - \left(b_1 \frac{\tilde{L}_z}{L_x}\right)^2} \\ 0 \\ 0 \end{pmatrix}, \quad \mathbf{e}_2^* = \begin{pmatrix} 0 \\ 1/\sqrt{1 - \left(b_2 \frac{\tilde{L}_z}{L_y}\right)^2} \\ 0 \end{pmatrix}, \quad \mathbf{e}_3^* = \begin{pmatrix} \frac{-b_1 \tilde{L}_z}{\sqrt{L_x^2 - b_1^2 \tilde{L}_z^2}} \\ \frac{-b_2 \tilde{L}_z}{\sqrt{L_y^2 - b_2^2 \tilde{L}_z^2}} \\ 1 \end{pmatrix}. \quad (\text{A.5})$$

In these definitions, b_1 and b_2 independently can take one of the two values 0 or $1/2$.

A.2 Intersection numbers

In this section, a mathematical derivation of the conjectured topological intersection number of two 2-dimensional branes, equation (4.18), on a T^3 will be given. The two 2-dimensional cycles (denoted by a and b) can be understood as 2-dimensional subtori of the original T^3 , i.e.

$$T_a^2, T_b^2 \subset T^3. \quad (\text{A.6})$$

Then the intersection of the two is a 1-torus T_I^1 times the collection of torsion points V_I of T^3 ,

$$T_a^2 \cap T_b^2 = T_I^1 \cdot V_I. \quad (\text{A.7})$$

The number of these torsion points $\#V_I$ corresponds to the topological intersection number (without orientation). A 2-torus most easily can be represented by a primitive vector in the reciprocal lattice of the original T^3 , equation (A.1). This means that the intersecting one-torus T_I^1 corresponds to the simultaneous solution of the two linear diophantine equations

$$\begin{aligned} m'_a x + n'_a y + p'_a z &= 0, \\ m'_b x + n'_b y + p'_b z &= 0. \end{aligned} \quad (\text{A.8})$$

A solution is given by

$$x = p'_b n'_a - p'_a n'_b, \quad y = m'_b p'_a - m'_a p'_b, \quad z = n'_b m'_a - m'_b n'_a. \quad (\text{A.9})$$

The number of torsion points therefore is given by

$$\#V_I = \text{gcd}(p'_b n'_a - p'_a n'_b, m'_b p'_a - m'_a p'_b, n'_b m'_a - m'_b n'_a) \quad (\text{A.10})$$

We define the (unoriented) topological intersection number between two 2-cycles on the T^3 by

$$I_{ab}^u \equiv \#V_I. \quad (\text{A.11})$$

There is no canonical mathematical way to attach a sign to this intersection number (although it is of course possible to do so by hand). This is easily understandable: an intersection is actually described by a vector (A.9) that has a well-defined direction in the 3-dimensional space (but no sign) and it can be reduced by the greatest common divisor of its components (A.10).

The standard unoriented intersection number of two 1-cycles on a 2-torus in our notation corresponds to the case when the two branes both wrap either the cycles $m'_a = m'_b = 0$ or $n'_a = n'_b = 0$, meaning that both vectors orthogonal to the branes lie either in the (y, z) - or (x, z) -plane of the reciprocal lattice. In this case, the sign of the oriented intersection number is simply established by choosing an oriented 'reference plane' and then by checking if the vector of the intersection is 'ingoing' or 'outgoing'. This reference plane is just given by the (x, z) - or (y, z) -plane itself, respectively.

Therefore, generally in the 3-dimensional case, we can only assign a sign to the intersection number (it will determine for instance the chirality of bifundamental representations) by explicitly choosing a 2-dimensional reference plane. In other words we have to specify what our internal space (2-dimensional per 3-torus) as opposed to the 4-dimensional spacetime exactly is.

A.3 Angle between branes

An oriented 2-cycle is characterized by a normal vector \vec{n} in the 3-dimensional reciprocal lattice. The angle between two such 2-cycles therefore can simply be obtained by the standard linear algebra formula

$$\alpha = \arccos \left(\frac{\vec{n}_a \cdot \vec{n}_b}{\|\vec{n}_a\| \|\vec{n}_b\|} \right). \quad (\text{A.12})$$

This angle is the smaller angle ($\leq \pi$) between the two normal vector, therefore it is unoriented in the sense that exchanging brane a with brane b does not change the angle in between them. It takes the explicit form

$$\alpha_i = \arccos \left(\frac{n_i^{a'} n_i^{b'} L_x^{i^2} (\tilde{L}_z^i)^2 + m_i^{a'} m_i^{b'} L_y^{i^2} (\tilde{L}_z^i)^2 + p_i^{a'} p_i^{b'} L_x^{i^2} L_y^{i^2}}{v_i^a v_i^b} \right), \quad (\text{A.13})$$

where

$$v_i^l \equiv \sqrt{n_i^{l'2} L_x^{i^2} (\tilde{L}_z^i)^2 + m_i^{l'2} L_y^{i^2} (\tilde{L}_z^i)^2 + p_i^{l'2} L_x^{i^2} L_y^{i^2}} \quad (\text{A.14})$$

is the 2-dimensional volume of the brane l on one 3-torus T_i^3 .

B Moduli space of a general T^3

A general T^k can be written as $\mathbb{R}^k / \mathbb{Z}^k$. This means that the dimension of the coset

$$GL(k, \mathbb{R}) / SO(k, \mathbb{R}) \quad (\text{B.1})$$

gives the dimension of the general T^k moduli space. The $GL(k, \mathbb{R})$ can be written as $\mathbb{R} \times SL(k, \mathbb{R})$, where \mathbb{R} is simply the determinant. According to the Iwasawa decomposition¹³, every element $g \in SL(k, \mathbb{R})$ can be written as

$$g = k a n, \quad (\text{B.2})$$

where k is an element of the maximal subgroup, which is given by $SO(k)$, a is an element of the maximal abelian subgroup, and n is an element of the nilpotent group. The maximal subgroup cancels against the $SO(k, \mathbb{R})$ of the coset (B.1), and remaining are only the determinant and the abelian subgroup, the elements of those together concretely can be understood as the elementary radii, and the nilpotent group, which can be understood as the angles between the elementary radii. For example, a T^2 has two elementary radii and one angle, a T^3 has three elementary radii and three angles, so altogether six moduli.

For the case of an orientifolded T^2 , the third modulus (explicitly the angle) is fixed by the orientifold plane to only discrete values, so only the two radii remain. A similar thing happens in the case of the T^3 : the orientifold projection fixes two of the three elementary torus angles to a discrete value. This is explained in more detail in section 3.1. This of course means that one angle remains unfixed. In the main text this angle is set by hand to 90 degrees, but the whole ansatz might be extended by also taking into account this additional angle in the future.

¹³I would like to thank A. Keurentjes for pointing me to this decomposition.

C Klein bottle lattice contributions

The Kaluza-Klein momenta and winding modes generally take the following form

$$\mathbf{P} = s_1/L_x \mathbf{e}_1^* + s_2/L_y \mathbf{e}_2^* + s_3/\tilde{L}_z \mathbf{e}_3^*, \quad (\text{C.1})$$

$$\mathbf{L} = \frac{1}{\alpha'} (r_1 L_x \mathbf{e}_1 + r_2 L_y \mathbf{e}_2 + r_3 \tilde{L}_z \mathbf{e}_3). \quad (\text{C.2})$$

The lattice contribution to the closed sting Hamiltonian is generally given by

$$\mathcal{H}_{\text{lattice, cl.}} = \frac{\alpha'}{2} (\mathbf{P}^2 + \mathbf{L}^2). \quad (\text{C.3})$$

In the discussed toroidal orientifold, equation (4.1) together with (4.2), the worldsheet parity transformation Ω acts as

$$\Omega : \quad \mathbf{P} \xrightarrow{\Omega} \mathbf{P}, \quad \mathbf{L} \xrightarrow{\Omega} -\mathbf{L}, \quad (\text{C.4})$$

whereas the reflection R acts as:

$$R : \quad P_x \xrightarrow{R} P_x, \quad P_y \xrightarrow{R} P_y, \quad P_z \xrightarrow{R} -P_z, \quad L_x \xrightarrow{R} L_x, \quad L_y \xrightarrow{R} L_y, \quad L_z \xrightarrow{R} -L_z. \quad (\text{C.5})$$

Therefore, the combined action is given by:

$$\Omega R : \quad P_x \xrightarrow{R} P_x, \quad P_y \xrightarrow{R} P_y, \quad P_z \xrightarrow{R} -P_z, \quad L_x \xrightarrow{R} -L_x, \quad L_y \xrightarrow{R} -L_y, \quad L_z \xrightarrow{R} L_z. \quad (\text{C.6})$$

Keeping just the invariant terms under (C.6), leads to the lattice contribution

$$\mathcal{H}_{\text{lattice, cl.}}^{\mathcal{K}} = \frac{\alpha'}{2} \left(\frac{s_1^2}{L_x^2} + \frac{s_2^2}{L_y^2} \right) + \frac{1}{2\alpha'} \left(r_3^2 \tilde{L}_z^2 \right). \quad (\text{C.7})$$

D Annulus lattice contributions

D.1 Case of vanishing angles between branes

After mapping the boundary conditions (2.24) for the open string to the corresponding closed string boundary conditions and additionally performing T-duality, one obtains

$$\begin{aligned} \partial_\tau X_i + \mathcal{B}_y^i \partial_\tau \tilde{Z}_i &= 0, \\ \partial_\tau Y_i - \mathcal{B}_x^i \partial_\tau \tilde{Z}_i &= 0, \\ \partial_\sigma \tilde{Z}_i - \mathcal{B}_y^i \partial_\sigma X_i + \mathcal{B}_x^i \partial_\sigma Y_i &= 0, \end{aligned} \quad (\text{D.1})$$

Using the fact that $\partial_\tau X_i = \alpha' \mathbf{P}_x^i$ and $\partial_\sigma X_i = \alpha' \mathbf{L}_x^i$ (similarly for Y_i and \tilde{Z}_i) and the definitions (C.1) and (C.2), we obtain the following set of equations in the D6-branes picture,

$$s_1^i + \frac{m_i}{N} r_3^i = 0, \quad (\text{D.2})$$

$$s_2^i + \frac{n_i}{N} r_3^i = 0, \quad (\text{D.3})$$

$$s_3^i - \frac{m_i}{N} r_1^i - \frac{n_i}{N} r_2^i = 0. \quad (\text{D.4})$$

These equations are linear diophantine equations and one has to be careful in order to find the most general integer solution and not just a subset, we will do this in some detail. The first two equations (D.2) and (D.3) have to be solved simultaneously, whereas (D.4) is independent from them and can be solved apart.

D.1.1 Solving (D.2) and (D.3)

Applying our redefinitions (3.10) of the main text, the first set takes the form

$$p'_i s_1^i + m'_i r_3^i = 0, \quad (\text{D.5})$$

$$p'_i s_2^i + n'_i r_3^i = 0, \quad (\text{D.6})$$

where n'_i, m'_i, p'_i are coprime. This fact implies that after defining

$$d_1^i = \gcd(p'_i, m'_i), \quad d_2^i = \gcd(p'_i, n'_i), \quad (\text{D.7})$$

that $\gcd(d_1^i, d_2^i) = 1$. Furthermore, we define

$$\hat{p}_i = d_1^i p'_i, \quad \hat{m}_i = d_1^i m'_i, \quad (\text{D.8})$$

and solve first for (D.5) in terms of \hat{p}_i and \hat{m}_i . The result is given by

$$s_1^i = \hat{m}_i k_i, \quad r_3^i = -\hat{p}_i k_i, \quad \text{where } k_i \in \mathbb{Z}. \quad (\text{D.9})$$

Similarly, after defining

$$\hat{p}_i = d_2^i p'_i, \quad \hat{n}_i = d_2^i n'_i, \quad (\text{D.10})$$

we find for (D.6) the solution

$$s_2^i = \hat{n}_i l_i, \quad r_3^i = -\hat{p}_i l_i, \quad \text{where } l_i \in \mathbb{Z}. \quad (\text{D.11})$$

These two results (D.9) and (D.11) are surely not the simultaneous solution of (D.5) and (D.6), but it should be contained as a subset. The most general result for r_3^i is given by the set

$$\left\{ -\frac{p_i}{d_1^i} k_i \right\} \cap \left\{ -\frac{p_i}{d_2^i} l_i \right\}. \quad (\text{D.12})$$

Therefore $d_1^i l_i = d_2^i k_i$ and thus

$$k_i = d_1^i w_i, \quad l_i = d_2^i w_i, \quad \text{where } w_i \in \mathbb{Z}. \quad (\text{D.13})$$

Therefore, the simultaneous solution for (D.5) and (D.6) is given by

$$s_1^i = m'_i w_i, \quad s_2^i = n'_i w_i, \quad r_3^i = -p'_i w_i, \quad \text{where } w_i \in \mathbb{Z}. \quad (\text{D.14})$$

D.1.2 Solving (D.4)

The third equation of the boundary conditions takes the following form,

$$p'_i s_3^i - m'_i r_1^i - n'_i r_2^i = 0, \quad (\text{D.15})$$

where again n'_i, m'_i, p'_i are coprime. This is a linear diophantine equation in three unknowns, the general solution is known to be¹⁴

$$\begin{aligned} r_1^i &= k_i \frac{n'_i}{d_i} + l_i p_i x_i, \\ r_2^i &= -k_i \frac{m'_i}{d_i} + l_i p_i y_i, \\ s_3^i &= l_i d_i, \end{aligned} \quad (\text{D.16})$$

where $k_i, l_i \in \mathbb{Z}$ are arbitrary integers, $d_i = \text{gcd}(n'_i, m'_i)$ and $x_i, y_i \in \mathbb{Z}$ have to fulfill the equation

$$m'_i x_i + n'_i y_i = d_i. \quad (\text{D.17})$$

x_i and y_i are not unique, but a different choice for them does not change the lattice as it just shifts the first lattice vector by a finite integer r , such that $k'_i = r + k_i$. On the other hand, no explicit solution for x_i and y_i can be given, it has to be determined case by case using for instance the Euclidean Divison algorithm. For the tadpole calculation this actually is no problem at all, because all terms including x_i, y_i and d_i cancel against each other, as we will see later.

The closed string lattice Hamiltonian, being defined by equation (C.3), takes the final form for the annulus amplitude

$$\begin{aligned} \mathcal{H}_{\text{lattice, cl.}}^A &= \frac{\alpha'}{2} \left(\frac{m_i'^2}{L_x^2} + \frac{n_i'^2}{L_y^2} + \frac{p_i'^2}{(\tilde{L}_z^i)^2} \right) w_i^2 + \frac{1}{2\alpha'} \left[\left(\frac{n_i'^2}{d_i^2} L_x^2 + \frac{m_i'^2}{d_i^2} L_y^2 \right) k_i^2 \right. \\ &\quad \left. + \left(\frac{n_i' p_i' x_i}{d_i} L_x^2 - \frac{m_i' p_i' y_i}{d_i} L_y^2 \right) 2k_i l_i + \left(p_i'^2 x_i^2 L_x^2 + p_i'^2 y_i^2 L_y^2 + d_i^2 (\tilde{L}_z^i)^2 \right) l_i^2 \right], \end{aligned} \quad (\text{D.18})$$

where the sum in the trace of the annulus amplitude runs over the three independent integers w_i, k_i and l_i (for every T_i^3). The corresponding open string Hamiltonian can be generally obtained via a modular transformation, using the Poisson resummation formula

$$\sum_{n \in \mathbb{Z}} e^{-\frac{\pi(n-c)^2}{t}} = \sqrt{t} \sum_{m \in \mathbb{Z}} e^{2\pi i c m} e^{-\pi m^2 t}. \quad (\text{D.19})$$

The second part of the Hamiltonian (D.18) comprises a technical complication because it contains a term that is bilinear in k_i and l_i . The solution is to write the second part of the Hamiltonian as a matrix of the form

$$\frac{1}{2\alpha'} \left[(k_i, l_i) \begin{pmatrix} c_1 & c_2 \\ c_2 & c_3 \end{pmatrix} \begin{pmatrix} k_i \\ l_i \end{pmatrix} \right],$$

¹⁴We thank the three mathematicians Joost van Hamel, Wouter Castryck and Hendrik Hubrechts to provide this result.

and then use the matrix generalization of the Poisson resummation,

$$\sum_{\vec{v} \in \mathbb{Z}^d} e^{-\frac{\pi}{t} \vec{v}^T \mathbf{S} \vec{v}} = t^{d/2} \sqrt{\det \mathbf{S}^{-1}} \sum_{\vec{w} \in \mathbb{Z}^d} e^{-\pi t \vec{w}^T \mathbf{S}^{-1} \vec{w}}. \quad (\text{D.20})$$

In this way we obtain the open string lattice Hamiltonian for the annulus amplitude

$$\begin{aligned} \mathcal{H}_{\text{lattice, op.}}^A = & \frac{1}{\alpha'} \left(\frac{m_i'^2}{L_x^2} + \frac{n_i'^2}{L_y^2} + \frac{p_i'^2}{(\tilde{L}_z^i)^2} \right)^{-1} \tilde{w}_i^2 + \frac{1}{4\alpha' \Delta} \left[\left(p_i'^2 x_i^2 L_x^2 + p_i'^2 y_i^2 L_y^2 \right. \right. \\ & \left. \left. + d_i^2 (\tilde{L}_z^i)^2 \right) d_i^2 \tilde{k}_i^2 + \left(m_i' p_i' y_i L_y^2 - n_i' p_i' x_i L_x^2 \right) 2\tilde{k}_i \tilde{l}_i d_i + \left(n_i'^2 L_x^2 + m_i'^2 L_y^2 \right) \tilde{l}_i^2 \right], \quad (\text{D.21}) \end{aligned}$$

with

$$\Delta \equiv d_i^2 \left(n_i'^2 L_x^2 (\tilde{L}_z^i)^2 + m_i'^2 L_y^2 (\tilde{L}_z^i)^2 + p_i'^2 L_x^2 L_y^2 \right). \quad (\text{D.22})$$

The sum in the amplitude runs over the independent integers $\tilde{w}_i, \tilde{k}_i, \tilde{l}_i \in \mathbb{Z}$. Most remarkable is the fact that indeed all terms containing x_i, y_i and d_i cancel against each other in $\sqrt{\det \mathbf{S}}$ that enters the tree channel tadpole cancellation condition. This happens after we have resubstituted equation (D.17).

D.2 Case of non-vanishing angles between branes

In contrast to the T^6 case, we still obtain a contribution from the lattice, simply because the intersection is one-dimensional and compact in the case of the T^9 . Compared to the case of a vanishing angle between the two branes, instead of (D.2)-(D.4) we have to solve the following set,

$$\begin{aligned} p_i^{a'} s_1^i + m_i^{a'} r_3^i &= 0, & p_i^{b'} s_1^i + m_i^{b'} r_3^i &= 0, \\ p_i^{a'} s_2^i + n_i^{a'} r_3^i &= 0, & p_i^{b'} s_2^i + n_i^{b'} r_3^i &= 0, \\ p_i^{a'} s_3^i - m_i^{a'} r_1^i - n_i^{a'} r_2^i &= 0, & p_i^{b'} s_3^i - m_i^{b'} r_1^i - n_i^{b'} r_2^i &= 0. \end{aligned} \quad (\text{D.23})$$

For now assume that the two primitive vectors defining the two branes a and b are not coinciding. Then, the most general solution to the set (D.23) is given by

$$\begin{aligned} s_1^i &= s_2^i = r_3^i = 0, \\ r_1^i &= \Lambda_i^{-1} (m_i^{b'} p_i^{a'} - m_i^{a'} p_i^{b'}) w_i, \\ r_2^i &= \Lambda_i^{-1} (p_i^{b'} n_i^{a'} - p_i^{a'} n_i^{b'}) w_i, \\ s_3^i &= \Lambda_i^{-1} (m_i^{b'} n_i^{a'} - m_i^{a'} n_i^{b'}) w_i, \end{aligned} \quad (\text{D.24})$$

where

$$\Lambda_i \equiv \text{gcd} (m_i^{b'} p_i^{a'} - m_i^{a'} p_i^{b'}, p_i^{b'} n_i^{a'} - p_i^{a'} n_i^{b'}, m_i^{b'} n_i^{a'} - m_i^{a'} n_i^{b'}). \quad (\text{D.25})$$

Therefore, we obtain the closed string lattice Hamiltonian

$$\begin{aligned} \mathcal{H}_{\text{lattice, cl.}}^{A_{ab}} = & \frac{1}{2\alpha' \Lambda_i^2} \left[\left(p_i^{b'} n_i^{a'} - p_i^{a'} n_i^{b'} \right)^2 L_x^2 \right. \\ & \left. + \left(m_i^{b'} p_i^{a'} - m_i^{a'} p_i^{b'} \right)^2 L_y^2 + \left(m_i^{b'} n_i^{a'} - m_i^{a'} n_i^{b'} \right)^2 (\tilde{L}_z^i)^2 \right] w_i^2. \quad (\text{D.26}) \end{aligned}$$

The sum in the amplitude runs over all integers $w_i \in \mathbb{Z}$. The open string Hamiltonian can be obtained in a similar way like in the last section by a modular transformation using equation(D.19), the result is given by

$$\mathcal{H}_{\text{lattice, op.}}^{\mathcal{A}_{ab}} = \alpha' \Lambda_i^2 \left[(p_i^{b'} n_i^{a'} - p_i^{a'} n_i^{b'})^2 L_x^{i2} + (m_i^{b'} p_i^{a'} - m_i^{a'} p_i^{b'})^2 L_y^{i2} + (m_i^{b'} n_i^{a'} - m_i^{a'} n_i^{b'})^2 (\tilde{L}_z^i)^2 \right]^{-1} \tilde{w}_i^2. \quad (\text{D.27})$$

E The NS-NS tadpole

For completeness, we will state the NS-NS tadpoles in this section. This can be done in two different ways: either directly from the one loop amplitude, which is exactly analogue to the treatment of the R-R-tadpole in section 4.1, or from the tree level scalar potential arising the Born-Infeld action. This derivation is more straightforward and equivalent to the other one, so it will be used here. The potential is derived in section 5.2, equation (5.19). All the NS-NS tadpoles can be obtained by simply differentiating the potential with respect to all the scalar fields that it depends on. This procedure leads to ten different tadpoles, the dilaton tadpole $\langle \phi \rangle_D \sim \partial V / \partial \phi$ and nine radion tadpoles, for instance $\langle L_x^i \rangle_D \sim \partial V / \partial L_x^i$.

Explicitly, they are given by

$$\langle \phi \rangle_D = \sum_{l=1}^k \tilde{N}_l v_1^l v_2^l v_3^l - 16 \sqrt{\frac{L_x^1 L_y^1 L_x^2 L_y^2 L_x^3 L_y^3}{\tilde{L}_z^1 \tilde{L}_z^2 \tilde{L}_z^3}}, \quad (\text{E.1})$$

$$\langle L_x^I \rangle_D = \sum_{l=1}^k \tilde{N}_l \frac{v_J^l v_K^l}{v_I^l} \left[\left(n_I^{(l)'} + b_2^I p_I^{(l)'} \right)^2 \frac{\tilde{L}_z^I}{L_y^I} - \left(m_I^{(l)'} + b_1^I p_I^{(l)'} \right)^2 \frac{\tilde{L}_z^I L_y^I}{L_x^I{}^2} + p_I^{(l)'}{}^2 \frac{L_y^I}{\tilde{L}_z^I} \right] - 16 \sqrt{\frac{L_y^I L_x^J L_y^J L_x^K L_y^K}{L_x^I \tilde{L}_z^I \tilde{L}_z^J \tilde{L}_z^K}}, \quad (\text{E.2})$$

$$\langle L_y^I \rangle_D = \sum_{l=1}^k \tilde{N}_l \frac{v_J^l v_K^l}{v_I^l} \left[\left(m_I^{(l)'} + b_1^I p_I^{(l)'} \right)^2 \frac{\tilde{L}_z^I}{L_x^I} - \left(n_I^{(l)'} + b_2^I p_I^{(l)'} \right)^2 \frac{\tilde{L}_z^I L_x^I}{L_y^I{}^2} + p_I^{(l)'}{}^2 \frac{L_x^I}{\tilde{L}_z^I} \right] - 16 \sqrt{\frac{L_x^I L_x^J L_y^J L_x^K L_y^K}{L_y^I \tilde{L}_z^I \tilde{L}_z^J \tilde{L}_z^K}}, \quad (\text{E.3})$$

$$\langle \tilde{L}_z^I \rangle_D = \sum_{l=1}^k \tilde{N}_l \frac{v_J^l v_K^l}{v_I^l} \left[\left(n_I^{(l)'} + b_2^I p_I^{(l)'} \right)^2 \frac{L_x^I}{L_y^I} + \left(m_I^{(l)'} + b_1^I p_I^{(l)'} \right)^2 \frac{L_y^I}{L_x^I} - p_I^{(l)'}{}^2 \frac{L_x^I L_y^I}{(\tilde{L}_z^I)^2} \right] + 16 \frac{1}{\tilde{L}_z^I} \sqrt{\frac{L_x^I L_y^I L_x^J L_y^J L_x^K L_y^K}{\tilde{L}_z^I \tilde{L}_z^J \tilde{L}_z^K}}, \quad (\text{E.4})$$

with $I, J, K \in \{1, 2, 3\}$ and $I \neq J \neq K \neq I$ and where v_i^l is defined by

$$v_i^l \equiv \sqrt{\left(n_i^{(l)'} + b_2^i p_i^{(l)'}\right)^2 \frac{L_x^i \tilde{L}_z^i}{L_y^i} + \left(m_i^{(l)'} + b_1^i p_i^{(l)'}\right)^2 \frac{L_y^i \tilde{L}_z^i}{L_x^i} + p_i^{(l)'}{}^2 \frac{L_x^i L_y^i}{\tilde{L}_z^i}}. \quad (\text{E.5})$$

F Modular function expansions

In the main text, the expansion of the following combination of modular functions in q is needed.

$$\begin{aligned} & \frac{-\vartheta^2 \begin{bmatrix} \frac{1}{2} \\ 0 \end{bmatrix} \vartheta \begin{bmatrix} \frac{1}{2} \\ -\kappa_1 \end{bmatrix} \vartheta \begin{bmatrix} \frac{1}{2} \\ -\kappa_2 \end{bmatrix} + \vartheta^2 \begin{bmatrix} 0 \\ 0 \end{bmatrix} \vartheta \begin{bmatrix} 0 \\ -\kappa_1 \end{bmatrix} \vartheta \begin{bmatrix} 0 \\ -\kappa_2 \end{bmatrix} - \vartheta^2 \begin{bmatrix} 0 \\ \frac{1}{2} \end{bmatrix} \vartheta \begin{bmatrix} 0 \\ \frac{1}{2} - \kappa_1 \end{bmatrix} \vartheta \begin{bmatrix} 0 \\ \frac{1}{2} - \kappa_2 \end{bmatrix}}{\vartheta \begin{bmatrix} \frac{1}{2} \\ \frac{1}{2} - \kappa_1 \end{bmatrix} \vartheta \begin{bmatrix} \frac{1}{2} \\ \frac{1}{2} - \kappa_2 \end{bmatrix}} \eta^6 \\ &= 2 \frac{\cos^2(\pi\kappa_1) + \cos^2(\pi\kappa_2) - 2 \cos(\pi\kappa_1) \cos(\pi\kappa_2)}{\sin(\pi\kappa_1) \sin(\pi\kappa_2)} \\ &+ 4 \frac{\cos^2(\pi\kappa_1) + \cos^2(\pi\kappa_2) + 8 \cos^2(\pi\kappa_1) \cos^2(\pi\kappa_2) - 6 \cos(\pi\kappa_1) \cos(\pi\kappa_2)}{\sin(\pi\kappa_1) \sin(\pi\kappa_2)} q + \mathcal{O}(q^2) \end{aligned} \quad (\text{F.1})$$

References

- [1] M. Berkooz, M. R. Douglas, and R. G. Leigh. *Branes Intersecting at Angles*. Nucl. Phys. B 480, 265 (1996), hep-th/9606139.
- [2] Ralph Blumenhagen, Mirjam Cvetič, Paul Langacker, and Gary Shiu. *Toward realistic intersecting D-brane models*. (2005), hep-th/0502005.
- [3] Tassilo Ott. *Aspects of stability and phenomenology in type IIA orientifolds with intersecting D6-branes*. (2003), hep-th/0309107.
- [4] Lars Gorlich. *$N = 1$ and non-supersymmetric open string theories in six and four space-time dimensions*. (2004), hep-th/0401040.
- [5] Fernando G. Marchesano Buznego. *Intersecting D-brane models*. (2003), hep-th/0307252.
- [6] Dieter Lust. *Intersecting brane worlds: A path to the standard model?* (2004), hep-th/0401156.
- [7] Robert H. Brandenberger and C. Vafa. *Superstrings In The Early Universe*. Nucl. Phys. B316, 391 (1989).
- [8] Augusto Sagnotti. *Open strings and their symmetry groups*. (1987), hep-th/0208020.

- [9] Ralph Blumenhagen, Lars Görlich, and Boris Körs. *A new class of supersymmetric orientifolds with D-branes at angles*. (1999), [hep-th/0002146](#).
- [10] Ralph Blumenhagen, Lars Görlich, and Boris Körs. *Supersymmetric 4D orientifolds of type IIA with D6-branes at angles*. JHEP 01, 040 (2000), [hep-th/9912204](#).
- [11] Ralph Blumenhagen, Lars Görlich, Boris Körs, and Dieter Lüst. *Noncommutative compactifications of type I strings on tori with magnetic background flux*. JHEP 10, 006 (2000), [hep-th/0007024](#).
- [12] Ralph Blumenhagen, Boris Körs, and Dieter Lüst. *Type I strings with F- and B-flux*. JHEP 02, 030 (2001), [hep-th/0012156](#).
- [13] C. Angelantonj, Ignatios Antoniadis, E. Dudas, and A. Sagnotti. *Type-I strings on magnetised orbifolds and brane transmutation*. Phys. Lett. B489, 223–232 (2000), [hep-th/0007090](#).
- [14] G. Aldazabal, S. Franco, Luis E. Ibanez, R. Rabadan, and A. M. Uranga. *D = 4 chiral string compactifications from intersecting branes*. J. Math. Phys. 42, 3103–3126 (2001), [hep-th/0011073](#).
- [15] Stefan Forste, Gabriele Honecker, and Ralph Schreyer. *Supersymmetric Z(N) x Z(M) orientifolds in 4D with D-branes at angles*. Nucl. Phys. B593, 127–154 (2001), [hep-th/0008250](#).
- [16] Stefan Forste, Gabriele Honecker, and Ralph Schreyer. *Orientifolds with branes at angles*. JHEP 06, 004 (2001), [hep-th/0105208](#).
- [17] C. Kokorelis, JHEP **0211** (2002) 027 [[arXiv:hep-th/0209202](#)].
- [18] M. Cvetič, G. Shiu and A. M. Uranga, Nucl. Phys. B **615**, 3 (2001) [[arXiv:hep-th/0107166](#)].
- [19] Shamit Kachru and John McGreevy. *Supersymmetric three-cycles and (super)symmetry breaking*. Phys. Rev. D61, 026001 (2000), [hep-th/9908135](#).
- [20] Angel M. Uranga. *Chiral four-dimensional string compactifications with intersecting D-branes*. Class. Quant. Grav. 20, S373–S394 (2003), [hep-th/0301032](#).
- [21] Gabriele Honecker and Tassilo Ott. *Getting just the supersymmetric standard model at intersecting branes on the Z(6)-orientifold*. Phys. Rev. D70, 126010 (2004), [hep-th/0404055](#).
- [22] Tassilo Ott. *Catching the phantom: The MSSM on the Z6-orientifold*. (2005), [hep-th/0505274](#).
- [23] Carlo Angelantonj and Augusto Sagnotti. *Open strings*. Phys. Rept. 371, 1–150 (2002), [hep-th/0204089](#).

- [24] Nima Arkani-Hamed, Savas Dimopoulos, and G. R. Dvali. *The hierarchy problem and new dimensions at a millimeter*. Phys. Lett. B429, 263–272 (1998), [hep-ph/9803315](#).
- [25] I. Antoniadis, N. Arkani-Hamed, S. Dimopoulos and G. R. Dvali, Phys. Lett. B **436**, 257 (1998) [[arXiv:hep-ph/9804398](#)].
- [26] D. N. Spergel et al. *First Year Wilkinson Microwave Anisotropy Probe (WMAP) Observations: Determination of Cosmological Parameters*. Astrophys. J. Suppl. 148, 175 (2003), [astro-ph/0302209](#).
- [27] Luis E. Ibanez, F. Marchesano, and R. Rabadan. *Getting just the standard model at intersecting branes*. JHEP 11, 002 (2001), [hep-th/0105155](#).
- [28] Ralph Blumenhagen, Boris Körs, Dieter Lüst, and Tassilo Ott. *The standard model from stable intersecting brane world orbifolds*. Nucl. Phys. B616, 3–33 (2001), [hep-th/0107138](#).
- [29] Ralph Blumenhagen, Boris Körs, Dieter Lüst, and Tassilo Ott. *Intersecting brane worlds on tori and orbifolds*. Fortsch. Phys. 50, 843–850 (2002), [hep-th/0112015](#).
- [30] T. E. Chupp et al. *Results of a new test of local Lorentz invariance: A Search for mass anisotropy in Ne-21*. Phys. Rev. Lett. 63, 1541–1545 (1989).
- [31] W. Fischler and Leonard Susskind. *Dilaton Tadpoles, String Condensates and Scale Invariance*. Phys. Lett. B171, 383 (1986).
- [32] Willy Fischler and Leonard Susskind. *Dilaton Tadpoles, String Condensates and Scale Invariance*. 2. Phys. Lett. B173, 262 (1986).
- [33] Joseph Polchinski and Yunhai Cai. *Consistency of Open Superstring Theories*. Nucl. Phys. B296, 91 (1988).
- [34] Carlo Angelantonj and Adi Armoni. *Non-tachyonic type 0B orientifolds, non-supersymmetric gauge theories and cosmological RG flow*. Nucl. Phys. B578, 239–258 (2000), [hep-th/9912257](#).
- [35] E. Dudas, G. Pradisi, M. Nicolosi, and A. Sagnotti. *On tadpoles and vacuum redefinitions in string theory*. Nucl. Phys. B708, 3–44 (2005), [hep-th/0410101](#).
- [36] E. Dudas and J. Mourad. *Brane solutions in strings with broken supersymmetry and dilaton tadpoles*. Phys. Lett. B486, 172–178 (2000), [hep-th/0004165](#).
- [37] Ralph Blumenhagen and Anamaria Font. *Dilaton tadpoles, warped geometries and large extra dimensions for non-supersymmetric strings*. Nucl. Phys. B599, 241–254 (2001), [hep-th/0011269](#).
- [38] E. Dudas, J. Mourad, and C. Timirgaziu. *On cosmologically induced hierarchies in string theory*. JCAP 0403, 005 (2004), [hep-th/0309057](#).

- [39] E. S. Fradkin and A. A. Tseytlin. *Nonlinear Electrodynamics from Quantized Strings*. Phys. Lett. B163, 123 (1985).
- [40] R. G. Leigh. *Dirac-Born-Infeld Action from Dirichlet Sigma Model*. Mod. Phys. Lett. A4, 2767 (1989).
- [41] C. P. Burgess, P. Martineau, F. Quevedo, G. Rajesh, and R. J. Zhang. *Brane antibrane inflation in orbifold and orientifold models*. JHEP 03, 052 (2002), [hep-th/0111025](#).
- [42] Ralph Blumenhagen, Boris Körs, Dieter Lüst, and Tassilo Ott. *Hybrid inflation in intersecting brane worlds*. Nucl. Phys. B641, 235–255 (2002), [hep-th/0202124](#).
- [43] D. Cremades, L. E. Ibanez, and F. Marchesano. *Yukawa couplings in intersecting D-brane models*. JHEP 07, 038 (2003), [hep-th/0302105](#).
- [44] M. Cvetič and I. Papadimitriou, Phys. Rev. D **68**, 046001 (2003) [Erratum-ibid. D **70**, 029903 (2004)] [[arXiv:hep-th/0303083](#)].
- [45] Akikazu Hashimoto and IV Taylor, Washington. *Fluctuation spectra of tilted and intersecting D-branes from the Born-Infeld action*. Nucl. Phys. B503, 193–219 (1997), [hep-th/9703217](#).
- [46] IV Taylor, Washington. *Lectures on D-branes, gauge theory and M(atrices)*. (1997), [hep-th/9801182](#).
- [47] Zurab Kakushadze, Gary Shiu, and S. H. Henry Tye. *Type IIB orientifolds with NS-NS antisymmetric tensor backgrounds*. Phys. Rev. D58, 086001 (1998), [hep-th/9803141](#).
- [48] Carlo Angelantonj. *Comments on open-string orbifolds with a non-vanishing B(ab)*. Nucl. Phys. B566, 126–150 (2000), [hep-th/9908064](#).
- [49] D. Lüst and S. Stieberger. *Gauge threshold corrections in intersecting brane world models*. (2003), [hep-th/0302221](#).
- [50] Michael B. Green and John H. Schwarz. *Anomaly Cancellation in supersymmetric d=10 Gauge Theory and Superstring Theory*. Phys. Lett. B149, 117–122 (1984).
- [51] Michael B. Green and John H. Schwarz. *Infinity Cancellations in SO(32) Superstring Theory*. Phys. Lett. B151, 21–25 (1985).
- [52] Ralph Blumenhagen, Volker Braun, Boris Körs, and Dieter Lüst. *Orientifolds of K3 and Calabi-Yau manifolds with intersecting D-branes*. JHEP 07, 026 (2002), [hep-th/0206038](#).
- [53] M. M. Sheikh Jabbari. *Classification of different branes at angles*. Phys. Lett. B420, 279–284 (1998), [hep-th/9710121](#).
- [54] N. Ohta and P. K. Townsend, Phys. Lett. B **418**, 77 (1998) [[arXiv:hep-th/9710129](#)].

- [55] Michael R. Douglas. *Topics in D-geometry*. *Class. Quant. Grav.* 17, 1057–1070 (2000), [hep-th/9910170](#).
- [56] J. Polchinski. *String theory. Vol. 2: Superstring theory and beyond*. Cambridge, UK: Univ. Pr. (1998) 531 p.
- [57] Tassilo Ott. *work in progress*.
- [58] Ralph Blumenhagen, Lars Görlich, and Tassilo Ott. *Supersymmetric intersecting branes on the type IIA T^6/\mathbb{Z}_4 orientifold*. *JHEP* 01, 021 (2003), [hep-th/0211059](#).